A model investigation of tropospheric ozone chemical tendencies in long-range transported pollution plumes

M. Auvray,[1] I. Bey,[1] E. Llull,[1,2] M. G. Schultz,[3] and S. Rast[3]

Received 30 January 2006; revised 10 August 2006; accepted 15 September 2006; published 9 March 2007.

[1] The impact of continental outflow on the ozone chemical tendencies (i.e., production and loss rates) is quantified in the North Atlantic and northwest Pacific regions using the GEOS-Chem and the MOZECH global models of chemistry and transport. The ozone tendencies simulated by these global models are compared to box model simulations constrained by observations in different regions and seasons. The two global models generally capture the seasonal and regional variations of the ozone tendencies. The largest discrepancies between the ozone tendencies from the box model and those from the global models are found in the lower troposphere of the eastern North Atlantic during the ACSOE campaign and are attributed to differences between chemical schemes and too strong NO_x concentrations in the global models. The background and plume (i.e., impacted by continental outflow) environments are differentiated over the oceanic areas using criteria based on simulated daily mean CO concentrations. The ozone tendencies in the plume environment differ from that in the background over the entire column in North Atlantic and northwest Pacific at all seasons. According to the models, net ozone production is enhanced by 2 to 6 ppbv/day in the boundary layer and by 1 to 3 ppbv/day in the upper troposphere, whereas the effect of pollution ranges from −1 ppbv/day to +1 ppbv/day in the middle troposphere (3–7 km), depending on the model used. The different responses of the two models are determined by differences in the water vapor distributions relative to those of pollutants in the plumes. In particular, GEOS-Chem tends to transport pollution in a drier sector of cyclones than MOZECH.

Citation: Auvray, M., I. Bey, E. Llull, M. G. Schultz, and S. Rast (2007), A model investigation of tropospheric ozone chemical tendencies in long-range transported pollution plumes, *J. Geophys. Res.*, *112*, D05304, doi:10.1029/2006JD007137.

1. Introduction

[2] In many regions of the world, ozone (O_3) concentrations are close to or even above the thresholds for plant damage or health effects [e.g., *Lövblad et al.*, 2004]. Elevated O_3 concentrations are associated with photochemical episodes which were initially thought to be local- and regional-scale problems. These issues have now to be considered on a hemispheric and even global scale as more and more scientific evidence is showing that transport of pollution can take place over long distances, such as across the Atlantic Ocean [e.g., *Parrish et al.*, 1993; *Fehsenfeld et al.*, 1996; *Collins et al.*, 2000; *Li et al.*, 2002a; *Wild and Akimoto*, 2001; *Trickl et al.*, 2003; *Auvray and Bey*, 2005] and the Pacific Ocean [e.g., *Jaffe et al.*, 1999, 2003; *Berntsen et al.*, 1999; *Yienger et al.*, 2000; *Fiore et al.*, 2002].

[3] Enhanced O_3 concentrations together with elevated carbon monoxide (CO) or nitrogen-containing compounds associated with long-range transport of pollution have been observed in the free troposphere over the North Atlantic in several cases [e.g., *Parrish et al.*, 1993; *Fehsenfeld et al.*, 1996]. Enhanced O_3 concentrations have been also reported at alpine sites [*Huntrieser et al.*, 2005] and in the lower troposphere of Europe [*Stohl and Trickl*, 1999; *Naja et al.*, 2003; *Trickl et al.*, 2003], but there is rarely a significant O_3 increase at surface stations associated with the arrival of such plumes over Europe [*Derwent et al.*, 1998]. *Guerova et al.* [2006] reported, for example, that long-range transport events from North America to Europe in summertime mainly occur during periods of unstable weather conditions and therefore do not coincide, in general, with the highest surface O_3 concentrations which typically occur during stable and sunny conditions. However, it has been suggested that long-range transport of pollutants across the Atlantic Ocean can substantially affect the mean O_3 concentrations over Europe [e.g., *Brönnimann et al.*, 2000, 2002; *Simmonds et al.*, 2004; *Ordóñez et al.*, 2005].

[1] Laboratoire de Modélisation de la Chimie Atmosphérique, Ecole Polytechnique Fédérale de Lausanne, Lausanne, Switzerland.
[2] Now at Department of Geosciences, University of Fribourg, Fribourg, Switzerland.
[3] Max Planck Institute for Meteorology, Hamburg, Germany.

0148-0227/07/2006JD007137

[4] While net photochemical formation of O_3 typically occurs near the source regions of precursor emissions, aircraft observations gathered over oceanic areas like the northwest Pacific have indicated that it can also take place over remote regions during long-range transport [e.g., *Davis et al.*, 1996, 2003; *Crawford et al.*, 1997; *Olson et al.*, 2001; *DiNunno et al.*, 2003; *Kondo et al.*, 2004; *Wild et al.*, 2004]. Similar results have been reported for the North Atlantic Ocean [*Wild et al.*, 1996; *Reeves et al.*, 2002]. It has been postulated that the continental outflow of O_3 and its precursors from the source regions into the remote atmosphere can lead to perturbations of the chemical environment in these regions. This subsequently affects the production and loss rates of O_3 and thus influences its chemical lifetime [e.g., *Schultz et al.*, 1998; *Honrath et al.*, 2004]. *Wild et al.* [2004] suggested that the impact of photochemical processes associated with such export events could have a substantial impact on O_3 levels on a global scale. Even though O_3 chemical tendencies (i.e., production and loss rates) have been discussed in several case studies with detailed analysis of aircraft observations, the overall contribution of the chemical perturbation due to long-range transport in remote areas to the global O_3 budget remains poorly quantified.

[5] The main objective of this paper is to examine how the O_3 tendencies over remote marine environments are modified by continental outflow. To this end we analyzed the characteristics of background and plume conditions over several oceanic regions using two global three-dimensional (3-D) chemistry transport models. Section 2 describes the two models and the simulations used in this study. In section 3, we examine to what extent the global models are capable of reproducing the O_3 production and loss rates obtained by box model simulations constrained by aircraft observations. The discrepancies between global and box models are then discussed with respect to the chemical mechanisms used as well as several environmental parameters. Section 4 discusses the impact of continental pollution outflow from North America into the North Atlantic Ocean over the annual course with special emphasis on spring and summer. The discussion is extended in section 5 for the northwest Pacific region. Summary and conclusions are provided in section 6.

2. Model Description and Simulation Setup

[6] The three-dimensional models used in this study are the chemistry transport model GEOS-Chem [*Bey et al.*, 2001a] and the chemistry-climate model MOZECH (S. Rast et al., Sensitivity of a chemistry climate model to changes in emissions and the driving meteorology, manuscript in preparation, 2007). A recent intercomparison between an ensemble of global chemistry transport models has shown that there are still significant differences in the simulated concentrations of trace gases and in the global tropospheric budget of O_3, even when the models use similar emission inventories for anthropogenic and biomass burning sources and are run for the same meteorological year [*Stevenson et al.*, 2006]. *Stevenson et al.* [2006] noted that the best agreement with observations is obtained with an average of all the model results. In the present study, we choose to employ two global models which include different physical parameterizations, transport algorithms, chemical schemes, and emission inventories. This allows us to explore the sensitivity of our results to different modeling tools and thus enhances the robustness of our results. Both models participated in the study of *Stevenson et al.* [2006] and they represent two rather different members of the ensemble. For example, the MOZECH model tends to have above-average O_3 concentrations. GEOS-Chem on the other hand generally agrees well with the ensemble mean, as well as with the observations, but tends to underestimate O_3 concentrations in the free troposphere of the northern midlatitudes. In the present work, two 1-year simulations (1997 and 2000) were performed with both models (after a 1-year spin-up), thereby taking into account variations in emissions and meteorology (GEOS-Chem) or only meteorological variations (MOZECH). In the following we briefly describe the main features of the two models.

2.1. GEOS-Chem

[7] The GEOS-Chem model [*Bey et al.*, 2001a], version 7–02 http://www.as.harvard.edu/chemistry/trop/geos/), is driven by assimilated meteorological fields from the Goddard Earth Observing System (GEOS) of the NASA Global Modeling and Assimilation Office (GMAO). For this study, the model was run with a horizontal resolution of 2° of latitude by 2.5° of longitude. The meteorological fields for the simulation of the years 1997 and 2000 are provided on 26 vertical levels up to 0.1 hPa and on 30 vertical levels up to 0.01 hPa, respectively. Advection and convection are computed every 15 min. Advection is computed with a flux form semi-Lagrangian method [*Lin and Rood*, 1996], and convection used the GEOS convective, entertainment and detrainment mass fluxes [*Allen et al.*, 1996a, 1996b]. A full mixing is assumed within the boundary layer. The model transports 24 tracers and includes more than 80 species and 300 chemical reactions based on *Horowitz et al.* [1998] to describe the O_x-NO_x-VOC photochemistry. Heterogeneous reactions on aerosols are taken into account as described by *Jacob* [2000] and *Martin et al.* [2003]. Aerosol fields are provided by the Global Ozone Chemistry Aerosol Radiation and Transport (GOCART) model [*Chin et al.*, 2002]. Photolysis frequencies are calculated with the FAST-J algorithm [*Wild et al.*, 2000] that accounts for cloud and aerosol optical depths and uses the Total Ozone Mapping Spectrometer/Solar Backscatter Ultraviolet (TOMS/SBUV) merged total O_3 column data sets.

[8] The inventory of anthropogenic emissions is similar to *Bey et al.* [2001a] except for the replacement of the European emissions with EMEP expert emissions following *Auvray and Bey* [2005]. To improve the emission estimates for specific years, the base 1985 inventory is scaled using CO_2 emission trends as described by *Bey et al.* [2001a]. NO_x emissions from international shipping (3.1 Tg N/yr) follow the EDGAR3.2 database with scaling for the year 2000 as described by *Dentener et al.* [2005]. Anthropogenic NO_x sources are released in the first two levels of the model, and all other anthropogenic sources only in the first level. Biomass burning emissions are from *Duncan et al.* [2003] with interannual variability being estimated from Along Track Scanning Radiometer (ATSR) firecounts. NO_x emissions from lightning are determined from cloud top height following the parameterization of *Price and Rind*

[1992] as implemented by *Wang et al.* [1998] with vertical profiles from *Pickering et al.* [1998], and account for about 6 Tg N/yr.

[9] Above the tropopause (diagnosed by a 2 K km^{-1} lapse rate), a simplified chemical representation is used, including production and loss of NO_y, CO and formaldehyde. Monthly mean production rates for NO_y are provided by the 2-D model of *Schneider et al.* [2000], along with NO_x/HNO_3 concentration ratios used to partition NO_y. This simplified stratospheric chemistry provides a source of NO_y to the troposphere. Transport of O_3 from the stratosphere is parameterized using the Synoz method (synthetic ozone) proposed by *McLinden et al.* [2000], leading to an O_3 cross-tropopause flux of about 550 Tg/yr.

2.2. MOZECH

[10] The "MOZART in ECHAM" (MOZECH) model is a newly developed fully coupled chemistry-climate model on the basis of the ECHAM5 general circulation model [*Roeckner et al.*, 2003] and the MOZART2 chemistry scheme including its numerical solver [*Horowitz et al.*, 2003]. For the purpose of this study the model is relaxed toward 6-hourly European Centre for Medium-Range Weather Forecasts (ECMWF) meteorological fields of surface pressure, temperature, vorticity, and divergence with time constants of 24h, 24h, 6h, and 48h, respectively. The resolution is T42L31, corresponding to a horizontal grid of about $2.8° \times 2.8°$ with 31 vertical levels from the surface to 10 hPa. Convection in ECHAM5 is parameterized according to *Tiedtke* [1989] and *Nordeng* [1994], and boundary layer mixing according to Monin-Obukhov [*Roeckner et al.*, 2003]. Further details on the physical and dynamical equations of ECHAM5 are given by *Roeckner et al.* [2003]. 63 species and 168 reactions are considered to describe the O_x-NO_x-VOC chemistry. Hydrolysis of N_2O_5 on sulfate aerosols is taken into account using climatological fields of sulfate aerosols from MOZART2 [*Horowitz et al.*, 2003]. Photolysis frequencies are computed on the basis of a precompiled multidimensional lookup table for zenith angle, total O_3 column, temperature, and surface albedo. An empirical cloud correction is applied as described by *Horowitz et al.* [2003].

[11] Anthropogenic emissions (including international ship traffic) are adapted from the model intercomparison experiment described by *Stevenson et al.* [2006] and are representative for the year 2000. Those emissions are released in the first model level. Biomass burning emissions are prescribed as 5-year mean monthly averages from 1997 to 2001 following *van der Werf et al.* [2003]. The production of NO_x from lightning is linked to the convective mass flux as described in *Grewe et al.* [2001] and are distributed following a C-shaped vertical profile. The annual source strength of lightning is of 3.3 Tg N/yr.

[12] Stratospheric NO_x, HNO_3, and CO concentrations are supplied from simulations of the 3-D MOZART3 model (D. E. Kinnison et al., Sensitivity of chemical tracers to meteorological parameters in the MOZART-3 chemical transport model, submitted to *Journal of Geophysical Research*, 2006). Stratospheric O_3 concentrations in MOZECH are prescribed as monthly mean zonal climatologies derived from observations [*Logan*, 1999; *Randel et al.*, 1998]. These concentrations are fixed at the topmost two model levels (pressures of 30 hPa and above). At other model levels above the tropopause, the simulated concentrations are relaxed toward these values with a relaxation time of 10 days. The net influx of O_3 from the stratosphere, diagnosed as the residual term in the global tropospheric O_3 budget, is 660 Tg/yr.

3. O_3 Chemical Tendencies: Model Intercomparison and Sensitivity Analysis

[13] In this section, we evaluate results from the two 3-D models using trace gas observations and O_3 tendencies from different aircraft field experiments. As direct measurements of the O_3 production and loss rates are not available, we have to rely on box model calculations which are constrained by observed concentrations [e.g., *Davis et al.*, 1996, 2003; *Jacob et al.*, 1996; *Crawford et al.*, 1997; *Jaeglé et al.*, 1998; *Schultz et al.*, 1999; *Reeves et al.*, 2002]. In order to obtain realistic concentrations for species or quantities not directly observed, the box models are typically run in a diurnal steady state mode; that is, the diurnal cycle of chemical reactions is repeated until a dynamic equilibrium has been reached. The results from such calculations can then be tested with independent observations such as NO/NO_2 ratio [e.g., *Schultz et al.*, 1999] or OH concentrations [e.g., *Wild et al.*, 2004]. While good agreement was reported for some studies, significant discrepancies were found in others, which could not always be reconciled [e.g., *Wild et al.*, 2004]. Nevertheless, O_3 production and loss rates obtained from those box models can provide interesting insights on the capability of the global models. Note however that 3-D models are in general superior to box models because they include air mass transport and, hence, "history" for each tracer.

[14] In the present work, we used observations and box model results provided by several aircraft experiments that were mainly dedicated to the sampling of continental outflow over oceanic regions. These include the Atmospheric Chemistry Studies in the Oceanic Environment (ACSOE) (eastern North Atlantic Ocean, April and September 1997, section 3.1), European Export of Precursors and Ozone by Long-range Transport (EXPORT) (continental Europe, summer 2000, section 3.2), Pacific Exploratory Mission–West A (PEM-West A) (North Pacific Ocean, fall 1991, section 3.3), and Transport and Chemical Evolution over the Pacific (TRACE-P) (North Pacific Ocean, spring 2001, section 3.3) campaigns. We limit the direct comparison of observed and simulated trace gas concentrations to those campaigns for which we performed dedicated model simulations (ACSOE in 1997 and EXPORT in 2000). We then compare photochemical O_3 tendencies derived from various box models constrained by trace gas observations to those obtained in our 3-D models for all campaigns. In addition, we perform a sensitivity study with the photochemical box model chem1d [*Jacob et al.*, 1996; *Jaeglé et al.*, 1998; *Schultz et al.*, 1999] to quantify the uncertainties in O_3 tendencies due to various parameters. This allows us to better interpret differences between the O_3 chemical tendencies estimated by the box models and those calculated in the global models.

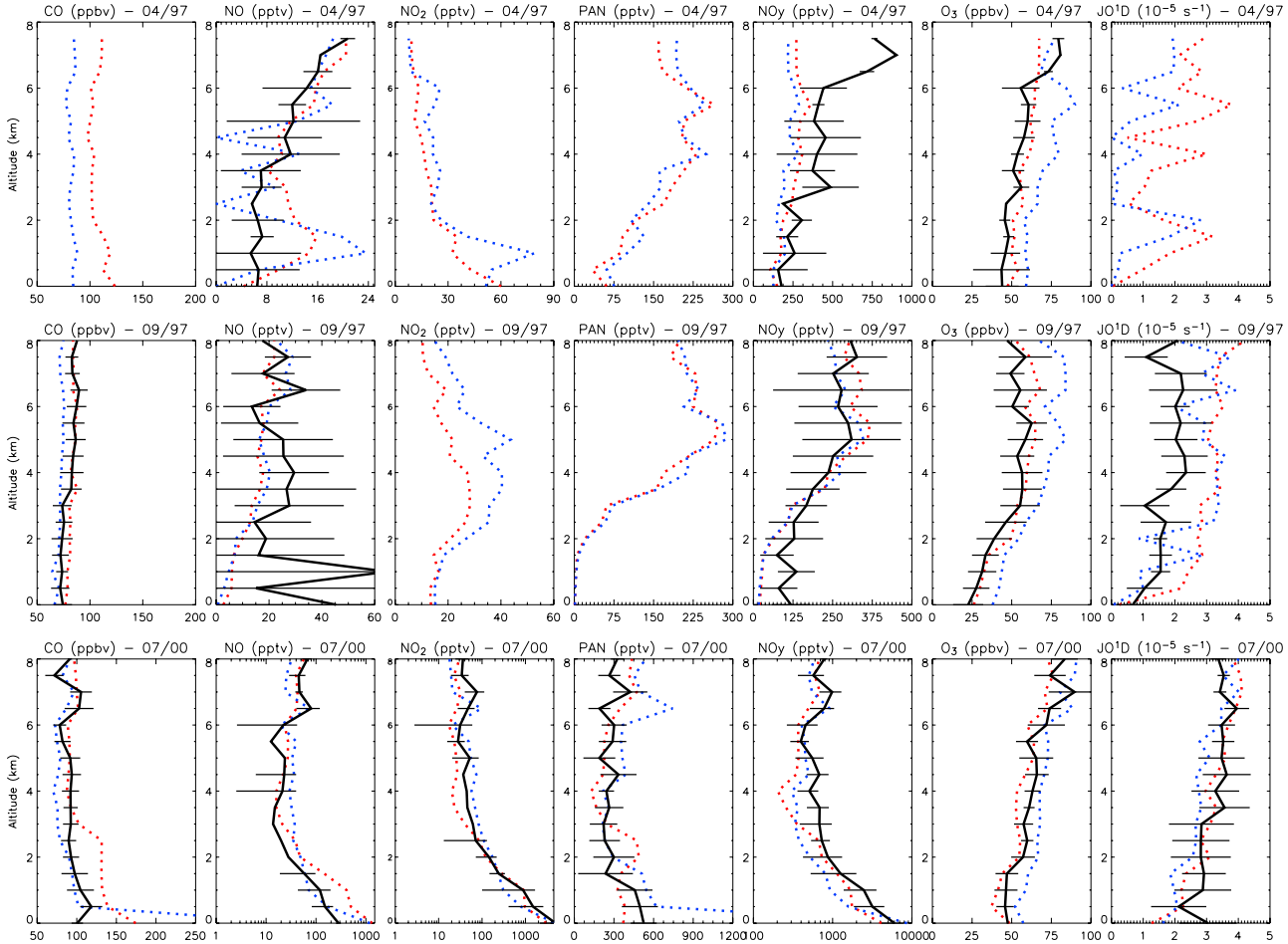

Figure 1. Observed (solid line) vertical profiles of the 5 min median CO, NO, NO_2, PAN, NO_y, O_3, and $J(O^1D)$ binned over 500 meters for (top and middle) the ACSOE and (bottom) the EXPORT campaigns. GEOS-Chem results (dotted red line) are sampled along the flight tracks at the time and location of the flights. MOZECH results (dotted blue line) are sampled every 5 min following the flight tracks, using model outputs every 3 hours. The horizontal bars show the observed standard deviations which reflect the variability found over the course of the three flights in April 1997, five flights in September 1997 and six flights in July-August 2000. CO, NO_2, and PAN observations are not available for April 1997, and NO_2 and PAN observations are not available for September 1997. For GEOS-Chem and MOZECH, NO_y correspond to the sum of NO_x and PAN (see details in the text, section 3.1.1). Logarithmic scale is used for NO, NO_2, and NO_y for EXPORT.

3.1. Eastern North Atlantic Ocean (ACSOE, Spring and Summer 1997)

[15] The ACSOE aircraft campaign took place in April (three flights) and September (five flights) 1997 to investigate the O_3 photochemistry over the North Atlantic Ocean [*Reeves et al.*, 2002; *Penkett et al.*, 2004]. While O_3 net production was generally found to be negative in the marine boundary layer and lower troposphere, *Reeves et al.* [2002] noticed a few cases with a positive net O_3 production (further referred to as netP O_3), which appeared to be associated either with recent ship emissions or with long-range transport of pollution from North America.

3.1.1. Comparison to Observed Trace Gases

[16] Figure 1 (top and middle) compare the median vertical profiles of different trace gas concentrations observed during ACSOE in April and September 1997 with the results from the GEOS-Chem and MOZECH models. CO concentrations were only measured in September, when they exhibit an almost height-independent profile and are well reproduced by the models. In the lower troposphere, above the boundary layer, the observed CO levels are closer to the MOZECH results, whereas GEOS-Chem performs better in the middle and upper troposphere. MOZECH CO concentrations are always lower than those simulated by GEOS-Chem, which may reflect excessive OH concentrations in MOZECH, and this is more pronounced in April than in September.

[17] *Reeves et al.* [2002] indicated that the air masses sampled in April had often a maritime origin, and we find that both GEOS-Chem and MOZECH tend to overestimate these low observed NO concentrations, especially in the lower troposphere. In September, enhancements in NO concentrations were observed in individual flights, which were attributed to ship plumes in the lower troposphere and

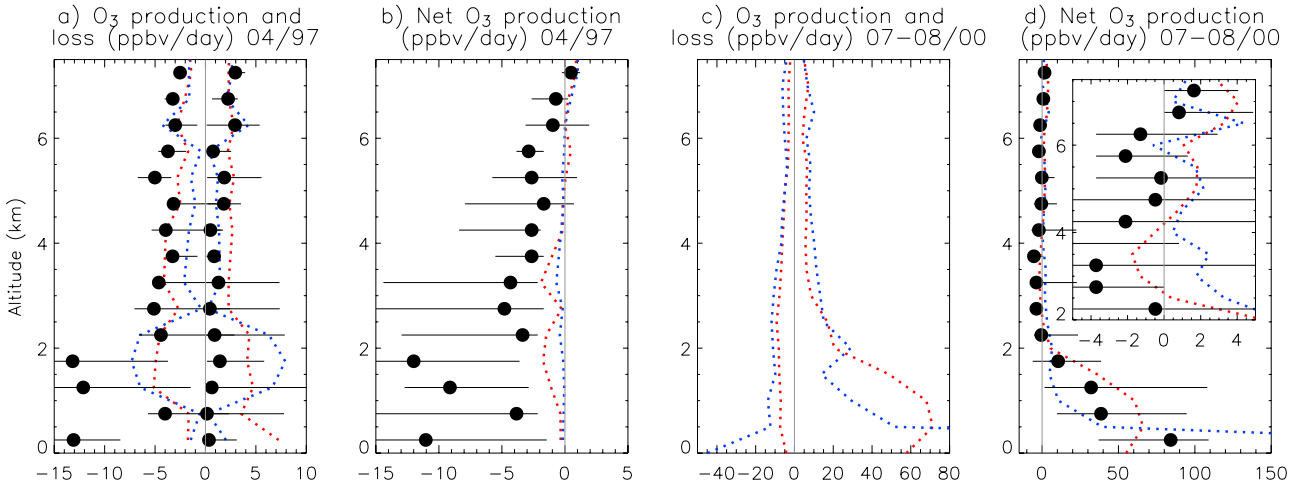

Figure 2. Vertical profiles of the median O_3 loss (negative value), production (positive value) rates, and net O_3 production binned over 500 meters altitude for (a and b) the ACSOE flights in April 1997 [*Reeves et al.*, 2002] and (c and d) the EXPORT flights in the summer 2000 [*Reeves and the EXPORT Team*, 2003] (in black). GEOS-Chem results (red dotted line) are sampled along the flight tracks at the time and location of the flights. MOZECH results (blue dotted line) are sampled every 5 min following the flight tracks, using model outputs every 3 hours. Horizontal bars represent observed 10th and 90th percentile. Units are in ppbv/day.

long-range transport in the middle troposphere [*Reeves et al.*, 2002]. In particular, at the altitude range of 4–6 km, high NO levels were associated with an episode of long-range transport of pollution from North America recorded on 14 September [*Reeves et al.*, 2002]. In September, both models tend to underestimate the median NO concentrations below 5 km. Although GEOS-Chem reproduces fairly well the enhancement in O_3 concentrations associated with the 14 September event [*Auvray and Bey*, 2005], the discrepancies in NO concentrations around 5 km may be related to the representation of that particular long-transport event. In the lower troposphere (below 2 km), the discrepancies may be due to the representation of NO emissions from ships in the global models. As emissions are smoothed out over the model grid boxes, the models tend to underestimate the elevated NO concentrations due to ship emissions observed in September while they tend to overestimate NO concentrations in clean regions (i.e., in April). Both models reproduce relatively well the observed NO concentrations in the upper troposphere.

[18] As measurements of NO_2 and PAN were not made in ACSOE, we can only compare the two models with each other. The simulated PAN concentrations generally agree well, whereas the differences are larger for NO_2. Here, MOZECH always simulates higher NO_2 concentrations than GEOS-Chem, implying higher levels of NO_x and a smaller NO/NO_2 ratio. This is consistent with the higher O_3 concentrations simulated by MOZECH (see below). As described by *Bauguitte* [2000] and *Penkett et al.* [2004], the NO_y observations do not include soluble species (e.g., HNO_3), but consist predominantly of NO_x and PAN. The simulated (NO_x + PAN) vertical profiles of the two models are again rather close to each other, and they generally agree well with the measurements. Exceptions are a significant underestimate of NO_y in the upper troposphere in April, and the underestimate in the boundary layer in September, which could again be explained by local ship emissions. The shape of the vertical O_3 profile is reproduced well by both models, but MOZECH overestimates O_3 by about 15 ppbv (30%) throughout the tropospheric column (except for altitudes above 6 km in April). The photolysis frequency of O_3 ($J(O^1D)$) was only measured in September, and it appears that both models overestimate $J(O^1D)$ by almost a factor of two during that season. In April, GEOS-Chem and MOZECH O_3 photolysis rates exhibit large variability below 5 km, which is consistent with the finding of *Reeves et al.* [2002] who derived $J(O^1D)$ from observed $J(NO_2)$.

3.1.2. Comparison to Box Model O_3 Chemical Tendencies

[19] Figures 2a and 2b show the comparison between the O_3 chemical tendencies from photochemical box model calculations reported by *Reeves et al.* [2002] with the 3-D model results for the April ACSOE flights. The box model used by *Reeves et al.* [2002] was constrained by observed temperature, pressure, NO_2 photolysis frequency, and observed concentrations of O_3, NO, H_2O, CO, H_2O_2, and CH_3OOH. CO concentrations were set to 133 ppbv (which is reasonably close to the GEOS-Chem values, but about a factor of two higher than MOZECH), while HCHO and CH_4 were set to 300 pptv and 1800 ppbv, respectively [*Reeves et al.*, 2002]. *Reeves et al.* [2002] found that the O_3 loss rates (median of the three April flights) decrease with altitude (reflecting drier air aloft) while O_3 production rates increase with altitude (reflecting higher NO concentrations in the upper troposphere). In their calculation, the crossover from negative to positive netP occurs at about 7 km of altitude.

[20] We find substantial differences between the box model results of *Reeves et al.* [2002] and our global model calculations (Figure 2a). Above 3 km, MOZECH captures the O_3 production rates rather well, but yields O_3 loss rates which are about a factor of two weaker than the box model. In contrast, GEOS-Chem reproduces well the O_3 loss rates between 3 and 5 km altitude, but overestimates the produc-

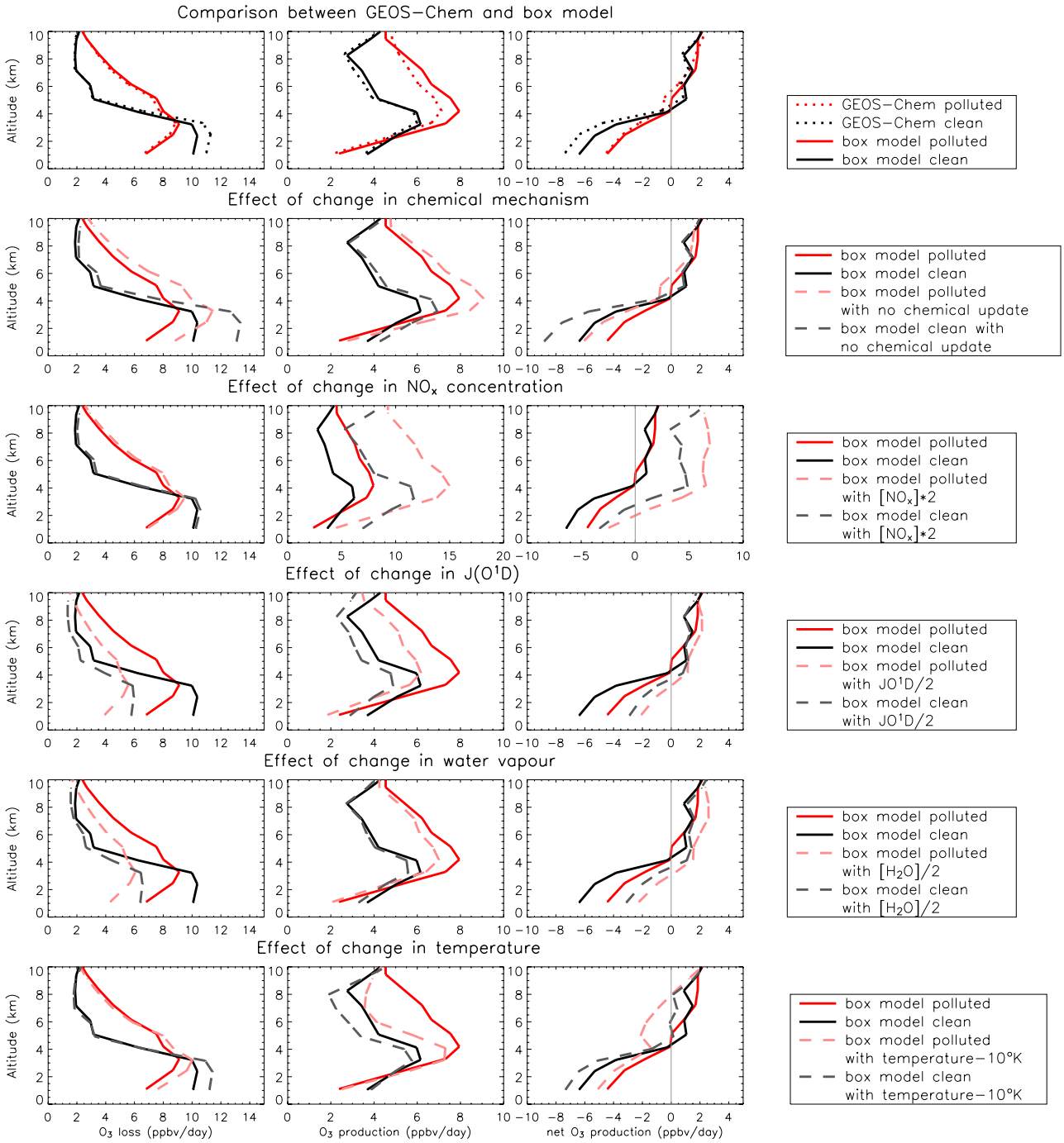

Figure 3. Vertical profiles of O_3 loss, O_3 production and net O_3 production (ppbv/day) as calculated by the standard version of chem1d (solid line) and GEOS-Chem (dotted line) for a polluted (red line) and clean case (black line) (first row). Subsequent rows show O_3 tendencies from different tests performed with chem1d to explore the sensitivity of chemical tendencies to various parameters (dashed lines).

tion rates by 20%. In the lower troposphere, both 3-D models exhibit substantially lower loss rates than the box model, but yield higher production rates, partly because the two global models overestimate observed NO. A deeper analysis of the GEOS-Chem and the box model results reveals that discrepancies in the O_3 production rates are due to both higher NO + HO_2 and NO + CH_3O_2 reaction rates in GEOS-Chem because of excessive NO concentrations, while discrepancies in the O_3 loss rates in the lower troposphere are mainly associated with O_3 photolysis because of excessive J(O^1D) (see Figure S1 in the auxiliary material)[1]. As a consequence of these discrepancies, the 3D models both show a much smaller (i.e., less negative) netP O_3 than the box model (Figure 2b).

[1]Auxiliary materials are available in the HTML. doi:10.1029/2006JD007137.

[21] Apart from differences in the trace gas distributions simulated by the various models (see section 3.1.1), there are also a few key reactions that are parameterized in different ways and can have a significant impact on the results, as further discussed in section 3.1.3. In addition, *Reeves et al.* [2002] do not consider heterogeneous chemistry on aerosols and wet deposition, whereas GEOS-Chem and MOZECH include the uptake of N_2O_5 and washout of HNO_3 and other soluble species. GEOS-Chem also considers the heterogeneous uptake of HO_2, which can have a significant effect on the radical chemistry [*Martin et al.*, 2003; *Tie et al.*, 2005]. Differences in the nonmethane hydrocarbon (NMHC) chemistry should be of little relevance, because NMHC concentrations are typically low over the remote ocean.

3.1.3. Sensitivity Analysis of O_3 Chemical Tendencies

[22] In order to better understand the differences between the global models and the observation-based box model, we performed a series of sensitivity experiments with the box model chem1d [*Jacob et al.*, 1996; *Jaeglé et al.*, 1998; *Schultz et al.*, 1999]. Chem1d was constrained with outputs from the GEOS-Chem model (temperature, pressure, NO_2 and O_3 photolysis frequencies, and concentrations of O_3, NO_x and related compounds ($NO + NO_2 + NO_3 + 2N_2O_5 + HNO_2 + HNO_4$), HNO_3, H_2O, CO, H_2O_2, CH_3OOH, CH_2O, C_2H_6, C_3H_8, and acetone). We ran two test cases representative of a plume and a clean environment over the North Atlantic Ocean in September 1997. The chem1d results are compared to that of GEOS-Chem in Figure 3 (first row). The agreement is remarkably good, although the O_3 production rates in GEOS-Chem are slightly lower than in the chem1d box model for the polluted case. This could be due to the use of a simplified peroxy radical chemistry in the global model and to the absence of HNO_3 deposition in the box model, the photolysis of HNO_3 being an additional source of NO_x.

[23] One experiment was conducted with the chem1d box model to explore the sensitivity of the O_3 chemical tendencies to some key reactions of the chemical mechanism. For example, we used the reaction rates of *DeMore et al.* [1997] and *Sander et al.* [2000] for the reactions O^1D with H_2O and O^1D with N_2 (used by *Reeves et al.* [2002] and also in MOZECH) instead of those from *Dunlea and Ravishankara* [2004] and *Ravishankara et al.* [2002] (used in GEOS-Chem and in the standard chem1d). We find that using the updated reaction rates decrease O_3 production and loss by about 9% and 19%, respectively, when averaged over the column (Figure 3, second row), indicating the importance of using similar reaction rates when interpreting differences between model results. This may explain the discrepancies between the loss rates simulated by GEOS-Chem and those derived from the ACSOE observations (see Figure 2a).

[24] Further tests were performed with the chem1d box model to investigate the sensitivity of O_3 chemical tendencies to additional parameters. The parameters we explored either differ between the 3-D model results and the inputs used in the box model calculations by *Reeves et al.* [2002] (e.g., NO_x concentrations, see section 3.1.1) or differ between polluted and background environment as discussed in section 4 (e.g., $J(O^1D)$, water vapor, temperature). If the NO_x concentrations are increased by a factor 2 (see for instance differences between observed and simulated NO_x during ACSOE for September 1997), the O_3 loss rates remain almost unaffected, whereas the production rates are enhanced almost linearly, increasing thus the netP O_3 by a similar amount (Figure 3, third row). This may explain the differences between the production rates simulated by GEOS-Chem and those derived from the ACSOE observations (see Figure 2). A decrease of a factor 2 in the photolysis rate $J(O^1D)$ reduces the loss and production rates by about 35% and 23%, respectively, which tends to increase the netP O_3 (Figure 3, fourth row). A similar effect is obtained when the water vapor concentration is decreased by a factor 2 (Figure 3, fifth row). As will be shown below (section 4.1), water vapor concentrations in polluted air masses are distinctly different between the two global models. Finally, a decrease of the temperature by 10 K over the whole tropospheric column, corresponding to the maximum difference between the background and polluted environments found in GEOS-Chem (see section 4) was tested. This leads to a column average change of about 5% and −9% for O_3 loss and production rates, respectively, thus causing a decrease of the netP O_3 (Figure 3, sixth row).

3.2. Continental Europe (EXPORT, Summer 2000)

[25] The EXPORT campaign took place in July and August 2000 over central and eastern Europe to investigate the fate of the European pollution [e.g., *Purvis et al.*, 2003]. Median profiles of observed CO, NO, NO_2, PAN, NO_y, and O_3 concentrations as well as $J(O^1D)$ photolysis frequencies [*Brough et al.*, 2003; *Gerbig et al.*, 1999] are shown in the bottom row of Figure 1 for the six flights of the C-130 British aircraft. Much higher levels of primary pollutants are typically observed in the boundary layer compared to the measurements of the ACSOE campaigns, reflecting the proximity of sources. The 3-D models are able to reproduce the profile shapes of all components rather well. However, neither model agrees well with observations in the boundary layer, and a more careful quantitative analysis reveals differences of up to a factor of four for boundary layer NO concentrations. MOZECH tends to yield lower NO and CO concentrations in the boundary layer than GEOS-Chem, but it shows rather high levels of precursors in the lowest model layer, which likely reflects differences in the schemes used for boundary layer mixing in the two models. The observed vertical O_3 profile resembles that of the April 1997 ACSOE campaign and falls between the results from the two models. Here GEOS-Chem tends to underestimate O_3 by about 10 ppbv especially in the middle troposphere while the opposite is true for MOZECH. The $J(O^1D)$ profile is well represented by both models with maximum errors of about 20%.

[26] The vertical profiles of the net O_3 production rates are qualitatively similar between the box model of *Reeves and the EXPORT Team* [2003] and the two 3-D models (Figure 2d). Below 2 km altitude, the netP O_3 is much higher over the EXPORT region than in the oceanic boundary layer. In the boundary layer (but except for the lowest model layer), MOZECH generally yields lower netP O_3 than the box model, whereas GEOS-Chem exhibits higher values. The shape of the three netP O_3 profiles remains rather similar above 2 km, but the two 3D models predict a neutral to slightly positive net O_3 tendency, while the median box model results show an O_3 loss of up to 5 ppbv/day. O_3 production and loss rates were not reported

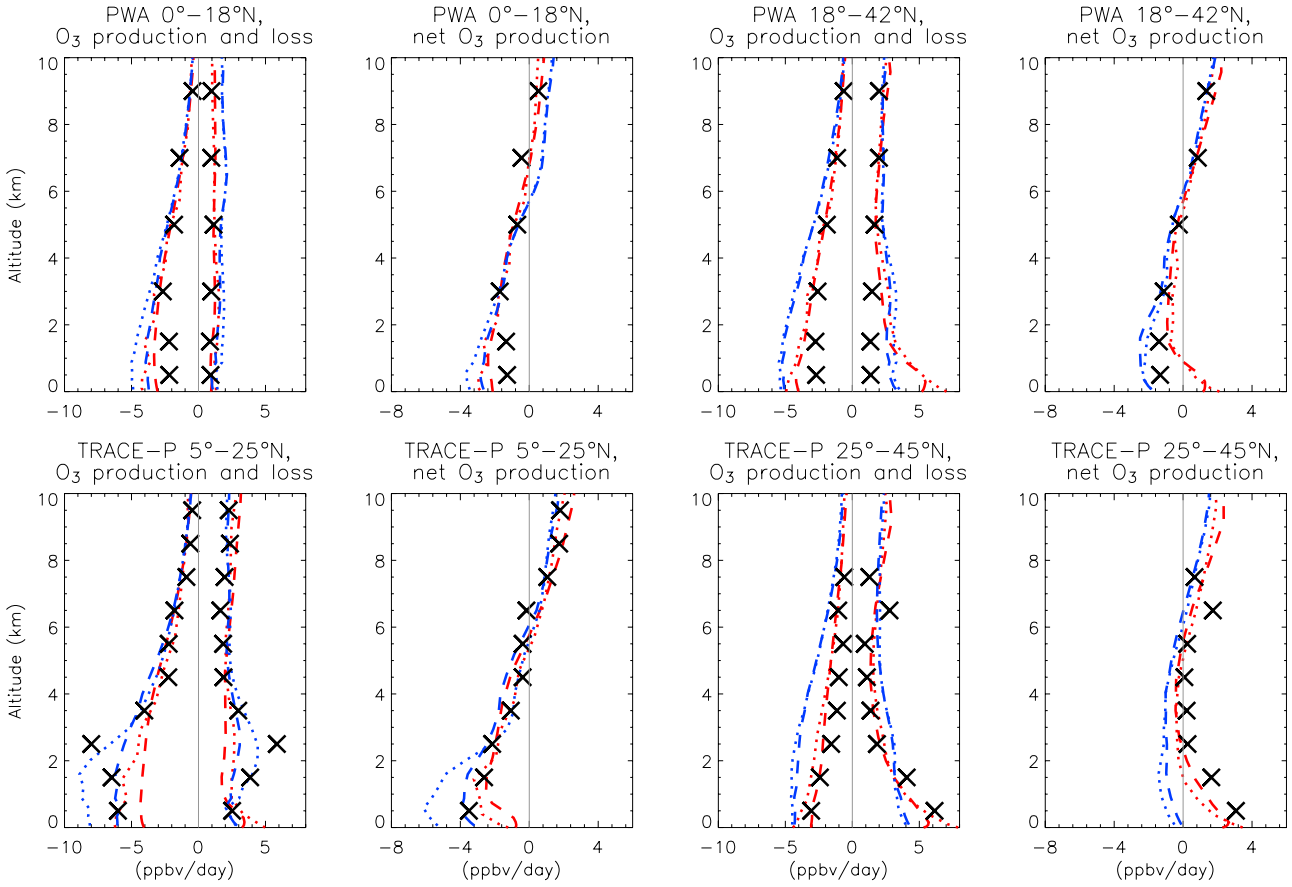

Figure 4. Vertical profiles of O_3 production and loss rate and net O_3 production rate in ppbv/day for the (top) PEM-WEST A and (bottom) TRACE-P campaigns. Black crosses indicate box model calculations for PEM-WEST A (PWA) and TRACE-P (J. Crawford, personal communication, 2005). Colored lines indicate GEOS-Chem (red) and MOZECH (blue) O_3 tendencies averaged over the southern (0–18°N) and northern (18–42°N) parts of the PEM-WEST A region (September-October) and over the southern (5–25°N) and northern (25–45°N) parts of the TRACE-P region (March-April). Model results are shown for two different meteorological years, 1997 (dotted lines) and 2000 (dashed lines).

individually by *Reeves and the EXPORT Team* [2003]. The 3-D models agree reasonably well with each other in the free troposphere while they differ by up to a factor 2 in the boundary layer and especially at the surface (Figure 2c).

3.3. North Pacific Ocean (PEM-West A, Summer/Fall 1991, and TRACE-P, Spring 2001)

[27] The PEM-West A and TRACE-P campaigns took place over the North Pacific rim in fall 1991 and spring 2001, respectively. Both campaigns reveal that the region north of 20°N is highly impacted by outflow of anthropogenic pollution from east Asia especially in spring when the outflow reaches a maximum, while the southern latitudes are more influenced by tropical/equatorial air masses [e.g., *Davis et al.*, 1996; *Crawford et al.*, 1997; *Jacob et al.*, 2003]. As we do not have detailed output from the 3-D models available for the years of the PEM-West A and TRACE-P campaigns, we restrict the evaluation of our results for the North Pacific to a comparison of simulated O_3 production and loss terms and netP O_3 with results from *Davis et al.* [1996, 2003] (note that we used in fact results from an updated version of the box model that includes a newer radiative transfer code and chemical scheme (J. Crawford, personal communication, 2005)). Global model results are presented for the years 1997 and 2000. Because of the different meteorological conditions and the changes in precursor emissions (and thus outflow concentrations), we do no expect perfect agreement between the box model and the two global models, but the profile shape and the magnitude of the terms can nevertheless provide insight into potential model biases. More detailed evaluations of GEOS-Chem over the North Pacific Ocean are reported elsewhere [*Bey et al.*, 2001b; *Liu et al.*, 2002; *Heald et al.*, 2003, 2004; *Hudman et al.*, 2004]. Generally, GEOS-Chem reproduces well the observed latitudinal and vertical gradients associated with continental outflow onto the North Pacific [*Bey et al.*, 2001b; *Hudman et al.*, 2004] but the stratospheric contribution to O_3 in the free troposphere appears to be underestimated in spring over the North Pacific [*Hudman et al.*, 2004].

[28] Figure 4 shows that the 3-D models can reproduce many features of the vertical profiles of the O_3 tendencies for the two campaigns. The box model (as well as the 3-D models) calculates higher production rates in the northern part than in the southern part of the regions, indicating a stronger influence of continental outflow north of 20°N

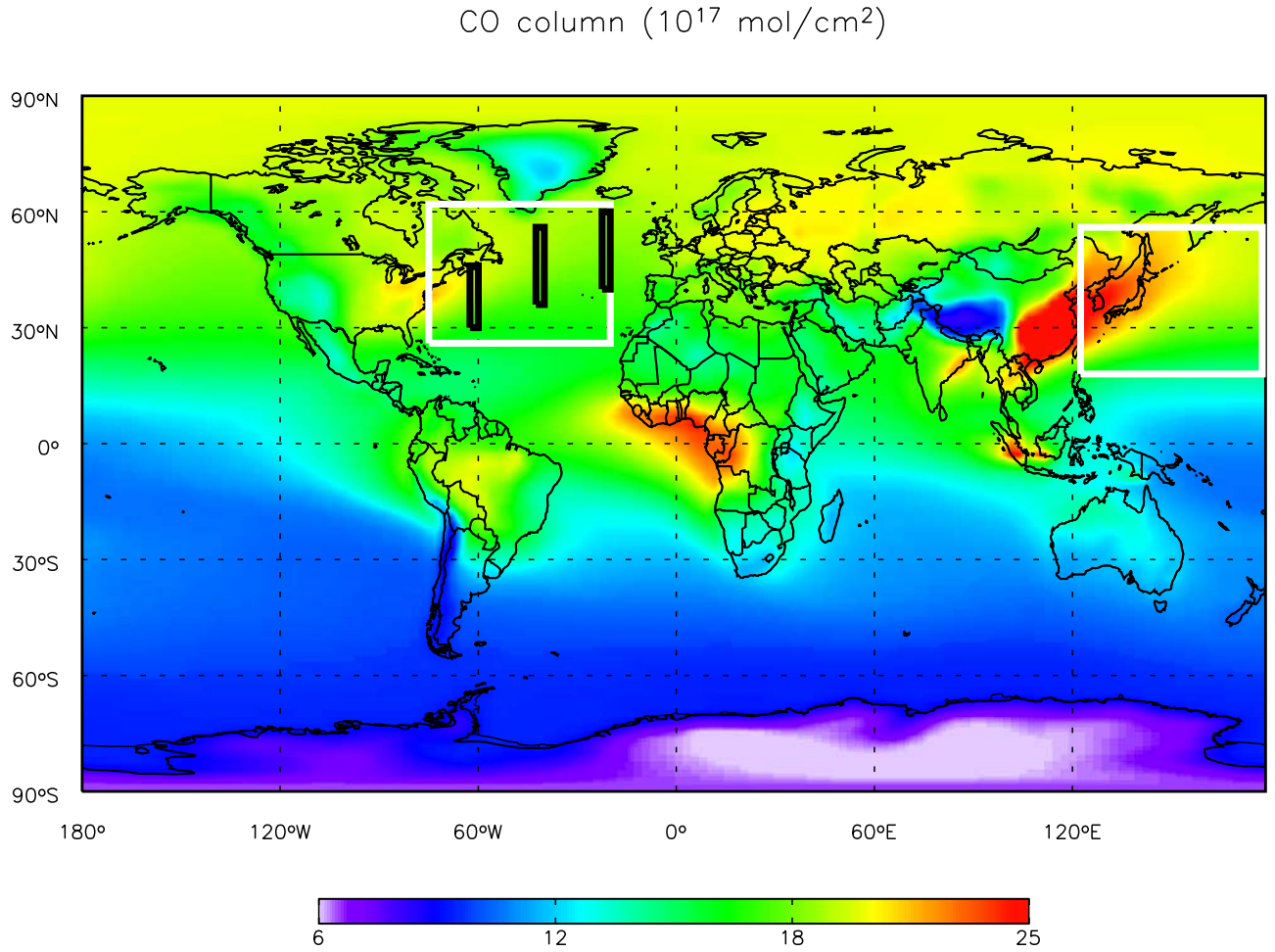

Figure 5. Geographical locations of the study regions described in this paper superimposed onto the annual mean GEOS-Chem CO column (10^{17} molecule/cm^2) integrated from the surface up to 180 mbar. North Atlantic region is 26–62°N, 75–20°W. Northwest Pacific region is 18–56°N, 122.5–177.5°E. The three black lines over the North Atlantic Ocean show the locations of the slices examined in section 4.

especially in spring. Both the production and loss rates appear to be higher during TRACE-P than during PEM-West A, especially in the boundary layer, reflecting the increasing photochemical activity in spring (as well as changes in O_3 precursor emissions over a decade, at least in the box model). Of particular interest is the small positive netP O_3, which is calculated by the box model over the entire column in the region and season more strongly affected by the continental outflow (e.g., in spring north of 25°N) [*Crawford et al.*, 1997; *Davis et al.*, 2003]. This is relatively well reproduced by GEOS-Chem. MOZECH however tends to have stronger O_3 loss rates over the Pacific that are likely associated with higher O_3 concentrations, and this leads to net O_3 destruction in that particular case.

3.4. Summary of the Model Intercomparison

[29] The two global models generally capture the seasonal and regional variations of O_3 chemical tendencies derived from different box models constrained with observations. Vertical profiles of the chemical tendencies are also fairly well reproduced. In particular, over the oceans, global and box models similarly find a shift from negative netP O_3 in the lower troposphere to positive netP O_3 in the middle/upper troposphere, even though the shift may occur at slightly different altitudes. Note, however, that a quantitative agreement between the global models and the box model could not always be reached. The largest discrepancies are seen in the lower troposphere of the eastern North Atlantic during the ACSOE campaign. We attribute these discrepancies to (1) different chemical schemes used in the models (as discussed in section 3.1.) and (2) overestimate of the observed NO_x concentrations (used as input in the box model) by the global models.

4. O_3 Chemical Tendencies in Polluted and Background Environment Over the North Atlantic

[30] This section examines how plumes transported over the North Atlantic Ocean affect O_3 tendencies in the free troposphere. We differentiate between the polluted environment (PE) and the background environment (BE) using daily mean CO concentrations of ocean grid boxes within the North Atlantic Ocean (see region in Figure 5). CO is

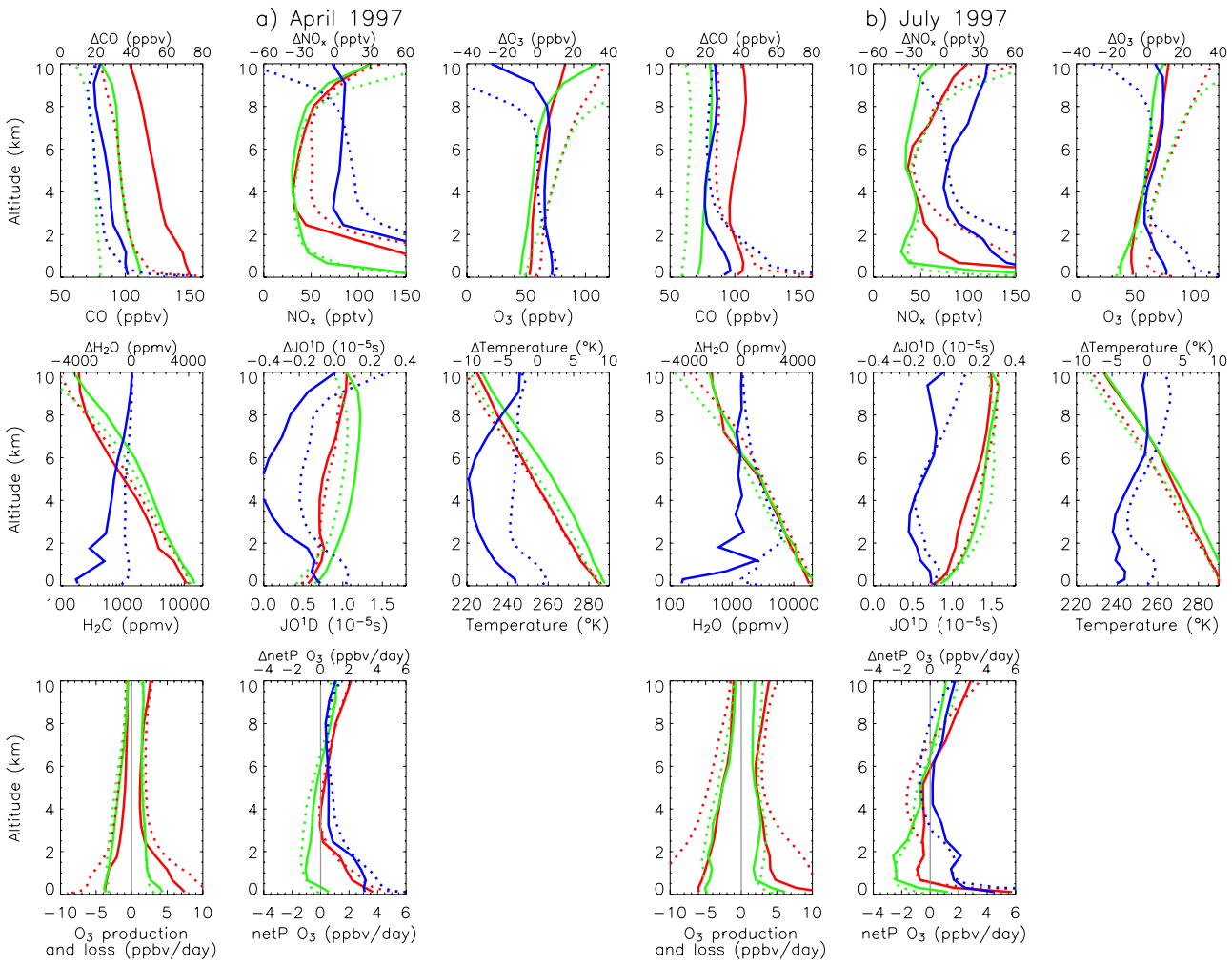

Figure 6. Simulated vertical profiles of CO (ppbv), NO_x (pptv), O_3 (ppbv), H_2O (ppmv), O_3 photolysis rate (10^{-5}s), temperature (K), and O_3 chemical tendencies (ppbv/day), for (a) April and (b) July 1997 over the North Atlantic Ocean. Green line indicates background environment (BE). Red line indicates plume environment (PE) (definitions in the text). Blue line indicates difference between the plume and the background environments (*x* axis for the difference between the two environments is given at the top of each panel). Solid line indicates GEOS-Chem. Dotted line indicates MOZECH.

emitted by incomplete combustion and is thus representative of both anthropogenic and biomass burning pollution. With a lifetime of a few months, CO is a good tracer of long-range transported plumes of various origins. BE is defined on each model level as the subset of grid box values for which the daily mean CO concentrations are lower than the regional monthly median CO concentration. PE is defined as the subset of grid boxes in the same region for which daily mean CO concentrations exceed the regional monthly median CO concentration plus one standard deviation. The choice of these criteria is somewhat arbitrary. However, sensitivity studies using different criteria (e.g., BE restricted to all grid box values for which CO is smaller than the median minus one standard deviation) yielded only little changes in the results which are negligible compared to the model uncertainties and the differences between the two models. The BE and PE statistics are computed separately for the two models. As the plumes are expected to evolve chemically as they are traveling, we first examined how the chemical tendencies differ between PE and BE in different longitudinal slices centered at 60°W, 40°W, and 20°W (Figure 5) along the north eastward path followed by most of the pollution plumes exported from the North American continent [e.g., *Trickl et al.*, 2003]. This test showed that considering an average over the entire oceanic region (rather than examining individual slices) also provides a reasonable picture of the O_3 tendencies and chemical behaviors in the two environments (see Figures S2 and S3). We thus discuss the seasonal variations of PE versus BE using various diagnosed quantities averaged over the entire oceanic region.

4.1. Spring

[31] Figure 6a shows vertical profiles of CO, NO_x, and O_3 concentrations in April 1997 for BE and PE conditions averaged over the North Atlantic area (see Figure 5 for the definition of the region and note that a land mask is applied so that only oceanic boxes are considered). As previously

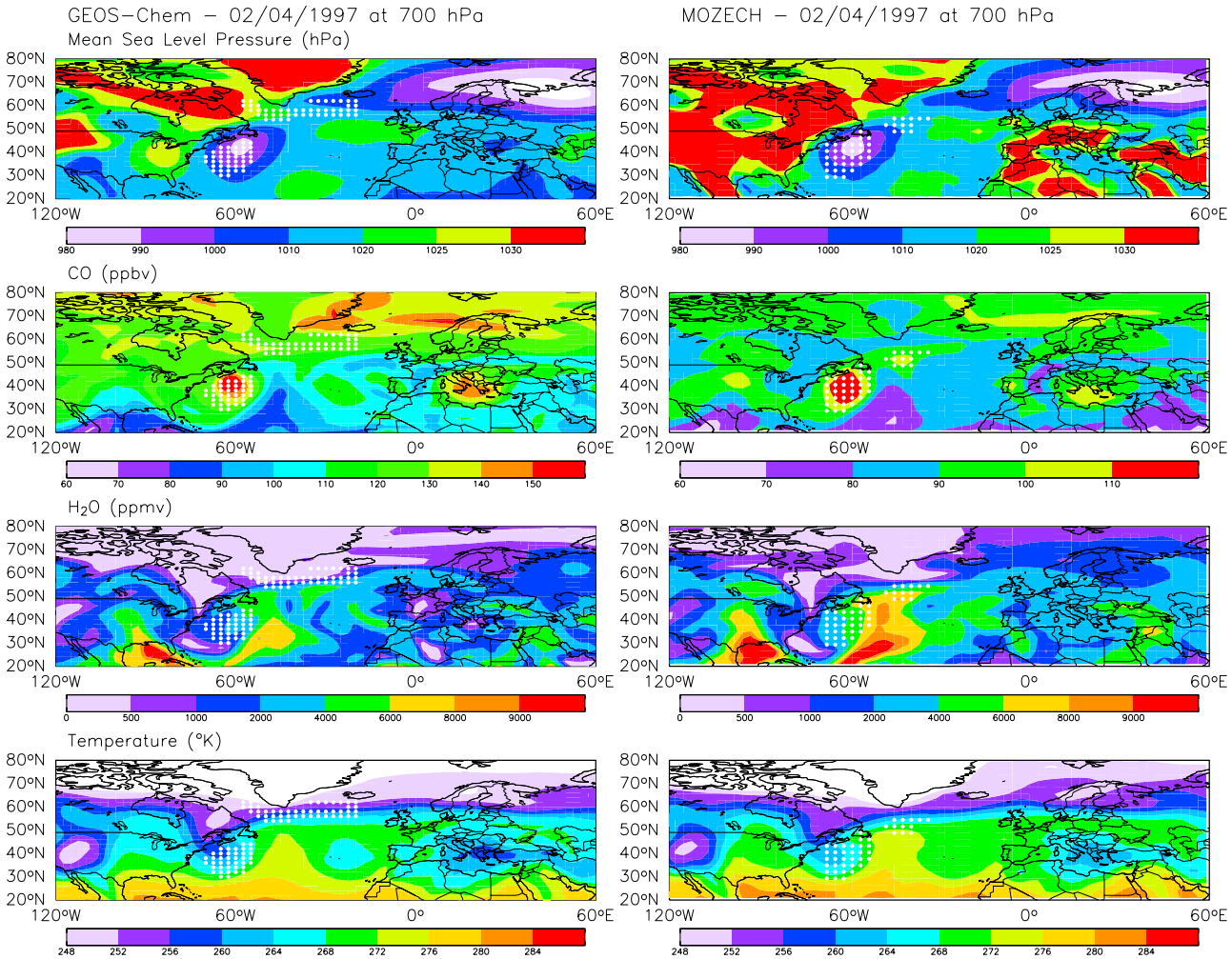

Figure 7. Mean sea level surface pressure (hPa), CO concentrations (ppbv), H_2O concentrations (ppmv) and temperature (°K) at 700 hPa for 2 April 1997 simulated with (left) GEOS-Chem and (right) MOZECH. White dots indicate the grid boxes identified as plumes (as defined in section 4) at 700 hPa. Note that the scales are different for CO.

mentioned (section 3), there are some substantial differences between the trace gas concentrations simulated by the two global models. CO concentrations are in general lower in MOZECH than in GEOS-Chem. On the other hand, MOZECH generally predicts higher O_3 concentrations than GEOS-Chem. The BE NO_x concentrations in the upper troposphere (above 8 km) are larger in MOZECH than in GEOS-Chem. Since the lightning sources in GEOS-Chem are twice as strong as in MOZECH, this is most probably due to different parameterizations used for representing the stratospheric flux of NO_y species (see section 2).

[32] Despite these model differences, the simulated differences in CO concentrations between the two environments (further referred to as $\Delta CO = CO_{PE} - CO_{BE}$) are similar for both models over the entire column (Figure 6a). This mainly reflects the various pathways which contribute to pollution export out of the U.S. boundary layer. Major pathways for North American pollution export are associated with mid-latitude cyclones and in particular with (1) rising air masses ahead of cold fronts (warm conveyor belt, WCB) which transport pollution at a large altitude range and (2) low-level air streams behind cold fronts (post cold front, PCF) [e.g., *Stohl and Trickl*, 1999; *Cooper et al.*, 2001, 2002a, 2002b; *Stohl*, 2001; *Li et al.*, 2002a; *Trickl et al.*, 2003]. Transport by cyclones occurs all year round, although it is less pronounced in summer [*Stohl*, 2001]. Note that pollution exported from the Asian continent is relatively well mixed over the North Atlantic, therefore its contribution likely falls in the BE rather than in the PE.

[33] ΔO_3 and ΔNO_x are positive in the lower and middle troposphere (Figure 6a). ΔO_3 (for the two models above 6 km) and ΔNO_x (for MOZECH above 8 km) become negative, reflecting an increase in stratospheric contribution with altitude. Stratospheric intrusions are generally associated with low CO concentrations and are therefore included in the BE class. We find an O_3 production efficiency per unit CO ($\Delta O_3/\Delta CO$) of about 0.22 and 0.25 ppbv/ppbv near the surface at 60°W, in GEOS-Chem and MOZECH, respectively. This is in good agreement with the value given by *Parrish et al.* [1998] for Sable Island in spring (0.19).

[34] Figure 6a also shows the vertical profile of water vapor concentrations, O_3 photolysis rates, and temperature

in BE and PE. GEOS-Chem predicts that PE is characterized by drier conditions than the surrounding background while in MOZECH, PE shows higher or similar water vapor levels than BE. This is especially seen at 60°W close to the region of export (Figure S2). A detailed analysis of daily scenes of surface pressure, water vapor, temperature fields, and plume location indicates that the two models tend to simulate the onset and evolution of transport episodes similarly and thus compare rather well in terms of plume locations, as illustrated in Figure 7. In spring these episodes are frequently associated with transient cyclones, as expected. We find, however, that GEOS-Chem has a tendency to transport the pollution in a drier sector of the cyclones, in comparison to MOZECH (Figure 7). These significantly different behaviors of the two models may reflect the use of different advection, convection, and boundary layer mixing schemes in the two models with potentially substantial consequences for the pollution redistribution with respect to export processes. However, this also may be related to the way water vapor transport is taken into account in the two models. While GEOS-Chem only interpolates between assimilated H_2O fields (updated every 6 hours), the GCM MOZECH includes a full parameterization of the hydrological cycle and advects water with the same routine as the chemical tracers. Both models indicate that PE is colder than BE, but the difference in temperature between the two environments is much larger in GEOS-Chem (up to 10 K) than in MOZECH (up to 5 K). Both models also predict enhanced presence of clouds in PE (not shown), which reduces the $J(O^1D)$ in PE by up to 30% and 20% in GEOS-Chem and MOZECH, respectively.

[35] The differences in water vapor and trace gases distributions have important implications for the O_3 chemical tendencies. O_3 loss rates are higher in PE than in BE in the boundary layer in MOZECH. This reflects higher O_3 concentrations and slightly higher O_3 photolysis rates in PE in this model. In contrast, GEOS-Chem shows O_3 loss rates lower in PE than in BE throughout the entire column. We attribute this different behavior in GEOS-Chem to a counterbalancing of enhanced O_3 in PE by the lower water vapor concentrations, temperature and O_3 photolysis rates (see also discussion in section 3.1.3 and Figure 3). In both models, O_3 production is enhanced in PE because of higher NO_x concentrations.

[36] Despite these different behaviors, both models predict a positive ΔnetP O_3 over the entire column, indicating the strong impact of long-range transport on chemical tendencies. The ΔnetP O_3 reaches about 2–3 ppbv/day. A positive ΔnetP O_3 is more clearly seen in the boundary layer and in the upper troposphere where the ΔNO_x is higher.

[37] As a consequence, the O_3 lifetime (i.e., the ratio of O_3 mass divided by O_3 loss) is affected by long-range transport in different ways in the two models. MOZECH predicts a small decrease of O_3 lifetime in PE (of 6 days on seasonal and regional average), while GEOS-Chem estimates an increase of 10 days on seasonal and regional average (27 days in the BE against 37 days in the PE). The largest increase in O_3 lifetime in GEOS-Chem is found in the middle and upper troposphere (38 days in BE against 62 days in PE), where O_3 has the greatest impact on radiative budget in the troposphere.

4.2. Summertime and Other Seasons

[38] Figure 6b shows the impact of long-range transport on O_3 chemical tendencies over the North Atlantic in summer. The impact of pollution export is also seen over the entire column as in spring. Pollution export out off the North American boundary layer in summer is governed by (1) cyclones (although they are less frequent in that season [*Stohl*, 2001]), (2) low-level zonal flows occurring between the well established Azores high and transient cyclones [e.g., *Guerova et al.*, 2006], and (3) deep convection, which occurs predominantly over central and southeastern U.S. and injects air directly at high altitudes (8 km and above) [e.g., *Thompson et al.*, 1994; *Horowitz et al.*, 1998; *Li et al.*, 2002a, 2005].

[39] The large enhancement seen in ΔCO in the lowest 3 km likely reflects these low-level outflow events while the slight "bump" seen in ΔCO at around 8 km (especially at 60°W, see Figure S3) is likely associated with deep convection. The effect of deep convection is more clearly seen in the ΔNO_x profiles (especially in GEOS-Chem) and is consistent with the findings of *Choi et al.* [2005] who reported evidence for simultaneous enhancements of NO_x and CO over the western North Atlantic Ocean associated with convective transport and lightning. Sensitivity tests without lightning performed with GEOS-Chem indicated that the contribution of lightning NO_x is more important in PE than BE. This is also true in MOZECH but to a lesser extent, as the global lightning NO_x emissions are lower by a factor of two as compared to GEOS-Chem.

[40] The two models predict different patterns in BE and PE, especially in the ΔNO_x vertical profiles, similarly to what was found for the spring season. In addition to the possible reason discussed in section 4.1, differences in the parameterization of lightning sources between the two models could explain some of the differences in NO_x between PE and BE in the upper troposphere. Note that the meteorological winds used in GEOS-Chem in the present work may suffer from excessive deep convection over the Caribbean and western North Atlantic [*Li et al.*, 2002b].

[41] GEOS-Chem predicts an O_3 production efficiency per unit CO ($\Delta O_3/\Delta CO$) of about 0.25 ppbv/ppbv at the surface at 60°W, which is comparable to the value of *Parrish et al.* [1998] at Sable Island in July (0.27) while MOZECH tends to overestimate this value (0.41).

[42] Substantial differences are also found between the water vapor profiles of the two models. As indicated in section 4.1, GEOS-Chem predicts drier air masses in PE (although this effect is limited to the first kilometer) while MOZECH predicts enhanced water vapor in PE. Figure S4 illustrates an event of low-level transport occurring at the periphery of the Azores High. This event is clearly seen in the two models, however the plumes tend to be located in more humid air masses in the case of MOZECH.

[43] Again, these differences in water vapor concentrations largely drive the differences in ΔnetP O_3 found between the two models. Because of the larger O_3 concentrations and water vapor levels in PE, MOZECH predicts a much higher O_3 loss in PE than in BE. This outweighs the enhanced O_3 production in PE (associated with elevated NO_x concentrations), resulting in a negative ΔnetP O_3 in the middle troposphere. In contrast, the O_3 loss rates in PE and

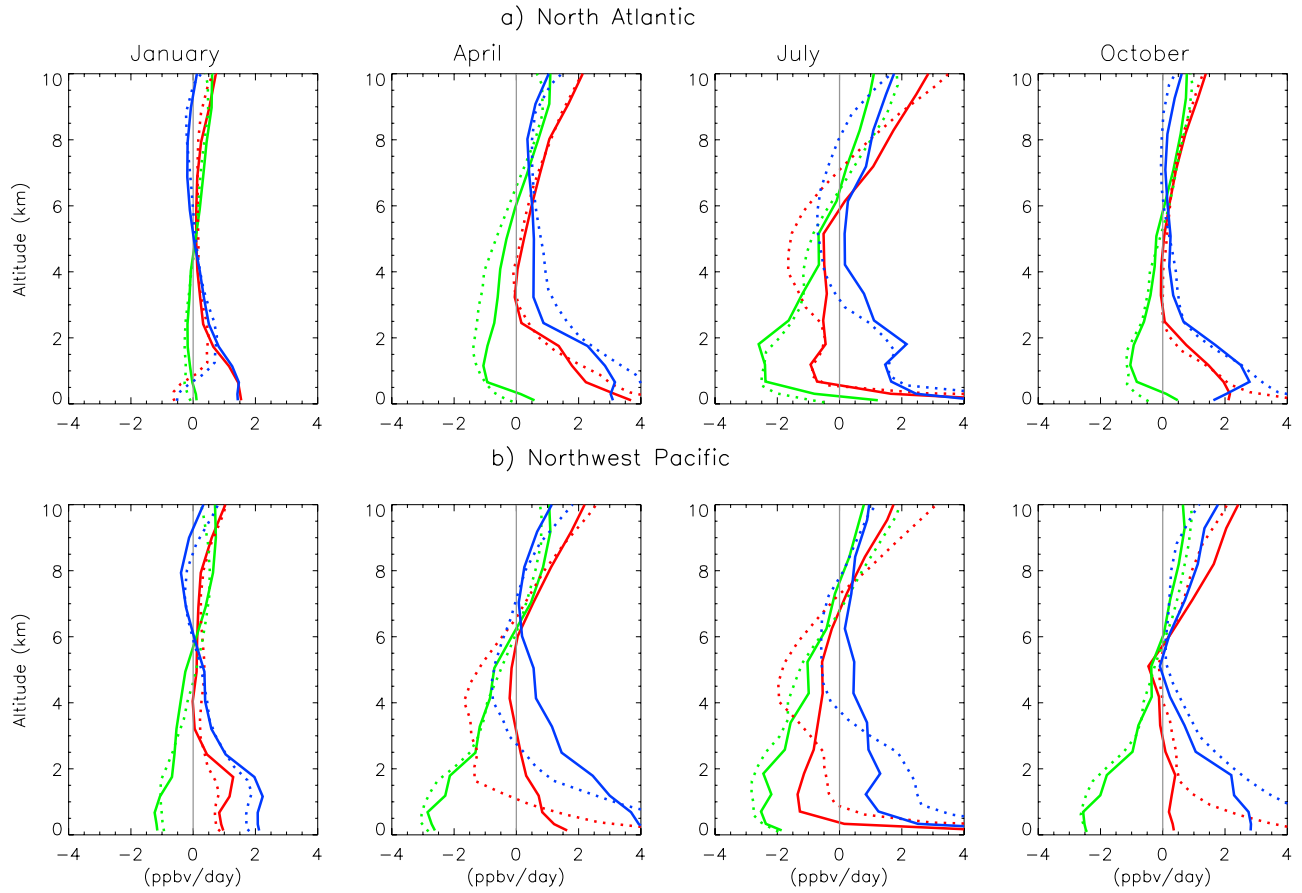

Figure 8. Simulated vertical profiles of net O_3 production (ppbv/day), for January, April, July, and October 1997 over the North Atlantic Ocean and the northwest Pacific Ocean. Green line indicates background environment. Red line indicates plume environment. Blue line indicates difference between the plume and the background environment (*x* axis for the difference between the two environments is given at the top of each figure). Solid line indicates GEOS-Chem. Dotted line indicates MOZECH.

BE are similar in GEOS-Chem (as the increase in O_3 concentrations is balanced by drier and colder air masses in plumes), and the increase in O_3 production associated with the ΔNO_x induces a positive ΔnetP O_3 over the entire column. The ΔnetP O_3 is at a maximum in the boundary layer and reaches up to 2–6 ppbv/day depending on the model.

[44] Finally, Figure 8a shows the netP O_3 for PE and BE for all seasons over the North Atlantic. The ΔnetP O_3 in fall resembles that in spring and only little additional O_3 formation is seen in winter, as expected.

5. Chemical Tendencies in the Northwest Pacific Region

[45] ΔnetP O_3 over the northwest Pacific is shown in Figure 8b. Continental outflow from Asia toward the Pacific Ocean occurs all year round with a maximum in spring [*Liu et al.*, 2003; *Liang et al.*, 2004]. Similarly to the North Atlantic, midlatitude cyclones [*Carmichael et al.*, 1998; *Yienger et al.*, 2000; *Stohl*, 2001; *Hannan et al.*, 2003] and convection [*Folkins et al.*, 1997; *Newell et al.*, 1997; *Bey et al.*, 2001b] are the two main mechanisms for export over the Pacific Ocean. The outflow is especially strong in spring as biomass burning pollution from Southeast Asia adds to the anthropogenic pollution and transport is most vigorous. The northwest Pacific exhibits similar patterns for the key species concentrations (see for example NO_x concentrations in Figure S5) and for the ΔNetP O_3 (Figure 8) as the North Atlantic, except that the ΔnetP O_3 is in general slightly higher over the Pacific. As before, the two models differ. GEOS-Chem predicts positive ΔnetP O_3 (up to 4 ppbv/day) over the entire column in both spring and summer, while MOZECH finds large positive ΔnetP O_3 up to 6 ppbv/day in the boundary layer but a negative value of 1 ppbv/day in the middle troposphere. As discussed above, these differences between the two models are likely related to the relative distributions of water vapor and trace gases in plumes. MOZECH predicts a positive ΔH_2O in spring, while GEOS-Chem predicts drier air masses in polluted environments (Figure S5).

6. Conclusion

[46] In this paper, we quantified the perturbation in O_3 chemical tendencies associated with continental outflow over the North Atlantic and northwest Pacific oceans as seen in two global models, namely GEOS-Chem and MOZECH. The global model results were first evaluated by comparison to observation-based O_3 production and loss

rates provided by several box models in various environments. Subsequently, the impact of continental pollution outflow on the chemical production and loss rates of O_3 over oceanic regions was investigated using CO concentration statistics as an indicator of plume locations. The two environments (i.e., polluted and background) were characterized in the two models in terms of tracer concentrations, water vapor content, temperature, and O_3 tendencies over the North Atlantic and the northwest Pacific for different seasons.

[47] Some substantial differences were found between the box model of *Reeves et al.* [2002] and the global models (especially over the eastern Atlantic Ocean). A sensitivity analysis suggested that these discrepancies mainly result from different reaction rates used in the chemical mechanisms (e.g., reactions O^1D with H_2O and O^1D with N_2), which significantly affect the O_3 loss rates, as well as from an overestimate of NO concentrations in the global models, which affect the O_3 production rates. Nevertheless, both models generally reproduce the seasonal and regional variations of the O_3 chemical tendencies rather well. For example, they capture the shift from negative to positive netP O_3 reported in the middle/upper troposphere in most of the cases and GEOS-Chem also reproduces the positive netP O_3 calculated in the entire column over the Pacific Ocean in spring associated with high continental outflow of both anthropogenic and biomass burning. MOZECH generally tends to show stronger O_3 loss rates than GEOS-Chem, which leads to a decrease of the netP O_3 in the middle troposphere over the northern Pacific in contrast to the photochemical box model results. Additional observation-based O_3 tendencies (and in particular those of the individual chemical pathways) would be useful to better evaluate global O_3-related chemical tendencies.

[48] The impact of plumes subject to long-range transport on the O_3 chemical tendencies is seen over the entire tropospheric column in both regions and in all seasons. The differences between the polluted and background environments reflect changes in various processes which contribute to O_3 photochemistry. In particular, O_3 production is enhanced when NO_x concentrations are higher, and O_3 loss is reduced (enhanced) if water vapor is reduced (enhanced) in the plumes. The two models, however, show significantly different behavior in both the polluted and background environments. GEOS-Chem predicts an enhancement of the netP O_3 in plumes over the entire column, which reaches a maximum of 3–4 ppbv/day in the boundary layer and up to 2 ppbv/day in the upper troposphere. MOZECH predicts in general a larger effect (up to 6 ppbv/day) in the boundary layer. In contrast, in the middle troposphere netP O_3 in MOZECH is reduced in the plume environment.

[49] An analysis of individual episodes indicated that the differences between the two models are related to differences in the water vapor distributions relative to those of the trace gases in the plumes. For example, over the North Atlantic in spring, GEOS-Chem tends to transport the pollution in a drier sector of the cyclones than MOZECH. We suggest that these discrepancies reflect differences between the two models in transport schemes (e.g., boundary layer mixing, convective mixing, advection) and in water vapor transport (online versus offline). Differences between the two models are also caused by the parameterizations of lightning sources and stratospheric fluxes. The differing water vapor and NO_x distributions in the two models result in different O_3 lifetimes in background and polluted environments. Further investigation is needed to quantify the chemical tendencies in individual long-range transport events. This could be based for example on observations gathered during Lagrangian aircraft experiments such as those performed in the framework of the International Consortium for Atmospheric Research on Transport and Transformation (ICARTT) program.

[50] Results were discussed in detail for the year 1997 but similar results are found for the year 2000 (see Figures S6–S8). *Parrish et al.* [2004] suggested that the chemical environment over the North Pacific changed significantly over the last 20 years and is now characterized by a less efficient O_3 destruction. Further studies are needed to quantify the change in netP O_3 due to the changes in anthropogenic emissions and to quantify the impacts of climate change (e.g., changes in water vapor levels and temperature).

[51] Our criterion to determine the spatial and temporal distribution of plumes is based on elevated CO concentrations, which can be indicative of anthropogenic or biomass burning events. It would be interesting to investigate whether the photochemical perturbation caused by plumes associated with biomass pollution differs from those with a more anthropogenic signature. Finally, the work presented here should be extended to also consider the impact of aerosols on the O_3 chemical tendencies in plumes. For example, *Price et al.* [2004] have shown that long-range transport events can contain elevated levels of both trace gases and aerosols. The latter can destroy trace gases and act on the UV flux, with significant impact on the O_3 photochemistry. In the simulations used in this work, aerosols were only accounted for on a climatological basis; that is, they were not transported along with the trace gases. Note also that, because aerosols are highly soluble, a better understanding of the discrepancies in terms of water vapor content in the plumes between the two models would be crucial to ensure a quantitative simulation of the export and subsequent long-range transport of aerosols.

[52] **Acknowledgments.** The GEOS-Chem model is managed by the Atmospheric Chemistry Modeling Group at Harvard University with support from the NASA Atmospheric Chemistry Modeling and Analysis Program. I.B. and M.A. wish to thank Claires Reeves for providing us with valuable information about her work and James Crawford for sending us updated box model results. I.B. and M.A. are grateful to Johannes Staehelin for commenting on an earlier version of that work conducted by Eric Llull and wish to thank Daniel Jacob for helpful discussions. S.R. and M.G.S. acknowledge funding from the EU under contract EVK2-CT-2002-00170 (RETRO) and helpful discussions with Johann Feichter and Stefan Kinne. We thank Gerd Folberth for helpful comments on the text. Finally, comments from two anonymous reviewers led to significant improvements in the manuscript and are greatly appreciated.

References

Allen, D. J., R. B. Rood, A. M. Thompson, and R. D. Hudson (1996a), Three-dimensional ^{222}Rn calculations using assimilated meteorological data and a convective mixing algorithm, *J. Geophys. Res.*, *101*(D3), 6871–6882.

Allen, D. J., P. Kasibhatla, A. M. Thompson, R. B. Rood, B. G. Doddridge, K. E. Pickering, R. D. Hudson, and S.-J. Lin (1996b), Transport-induced interannual variability of carbon monoxide determined using a chemistry and transport model, *J. Geophys. Res.*, *101*(D22), 28,655–28,670.

Auvray, M., and I. Bey (2005), Long-range transport to Europe: Seasonal variations and implications for the European ozone budget, *J. Geophys. Res.*, *110*, D11303, doi:10.1029/2004JD005503.

Bauguitte, S. (2000), A study of tropospheric reactive nitrogen oxides in the North Atlantic region, Ph.D. thesis, Univ. of East Anglia, Norwich, U. K.

Berntsen, T. K., S. Karlsdottir, and D. A. Jaffe (1999), Influence of Asian emissions on the composition of air reaching the north western United States, *Geophys. Res. Lett.*, *26*, 2171–2174.

Bey, I., D. J. Jacob, R. M. Yantosca, J. A. Logan, B. D. Field, A. M. Fiore, Q. Li, H. Liu, L. J. Mickley, and M. Schultz (2001a), Global modeling of tropospheric chemistry with assimilated meteorology: Model description and evaluation, *J. Geophys. Res.*, *106*, 23,073–23,095.

Bey, I., D. J. Jacob, J. A. Logan, and R. M. Yantosca (2001b), Asian chemical outflow to the Pacific in spring: Origins, pathways, and budgets, *J. Geophys. Res.*, *106*, 23,097–23,114.

Brönnimann, S., E. Schuepbach, P. Zanis, B. Buchmann, and H. Wanner (2000), A climatology of regional background ozone at different elevations in Switzerland (1992–1998), *Atmos. Environ.*, *34*, 5191–5198.

Brönnimann, S., B. Buchmann, and H. Wanner (2002), Trends in near-surface ozone concentrations in Switzerland: The 1990s, *Atmos. Environ.*, *36*, 2841–2852.

Brough, N., et al. (2003), Intercomparison of aircraft instruments on board the C-130 and Falcon 20 over southern Germany during EXPORT 2000, *Atmos. Chem. Phys.*, *3*, 2127–2138.

Carmichael, G. R., I. Uno, M. J. Phadnis, Y. Zhang, and Y. Sunwoo (1998), Tropospheric ozone production and transport in the springtime in east Asia, *J. Geophys. Res.*, *103*, 10,649–10,672.

Chin, M., P. Ginoux, S. Kinne, O. Torres, B. Holben, B. N. Duncan, R. V. Martin, J. A. Logan, A. Higurashi, and T. Nakajima (2002), Tropospheric aerosol optical thickness from the GOCART model and comparisons with satellite and sunphotometer measurements, *J. Atmos. Sci.*, *59*, 461–483.

Choi, Y., Y. Wang, T. Zeng, R. V. Martin, T. P. Kurosu, and K. Chance (2005), Evidence of lightning NO_x and convective transport of pollutants in satellite observations over North America, *Geophys. Res. Lett.*, *32*, L02805, doi:10.1029/2004GL021436.

Collins, W. J., D. S. Stevenson, C. E. Johnson, and R. G. Derwent (2000), The European regional ozone distribution and its links with the global scale for the years 1992 and 2015, *Atmos. Environ.*, *34*, 255–267.

Cooper, O. R., J. L. Moody, D. D. Parrish, M. Trainer, T. B. Ryerson, J. S. Holloway, G. Hübler, F. C. Fehsenfeld, S. J. Oltmans, and M. J. Evans (2001), Trace gas signatures of the airstreams within North Atlantic cyclones: Case studies from the North Atlantic Regional Experiment (NARE'97) aircraft intensive, *J. Geophys. Res.*, *106*, 5437–5456.

Cooper, O. R., J. L. Moody, D. D. Parrish, M. Trainer, T. B. Ryerson, J. S. Holloway, G. Hübler, F. C. Fehsenfeld, and M. J. Evans (2002a), Trace gas composition of midlatitude cyclones over the western North Atlantic Ocean: A conceptual model, *J. Geophys. Res.*, *107*(D7), 4056, doi:10.1029/2001JD000901.

Cooper, O. R., J. L. Moody, D. D. Parrish, M. Trainer, J. S. Holloway, G. Hübler, F. C. Fehsenfeld, and A. Stohl (2002b), Trace gas composition of midlatitude cyclones over the western North Atlantic Ocean: A seasonal comparison of O_3 and CO, *J. Geophys. Res.*, *107*(D7), 4057, doi:10.1029/2001JD000902.

Crawford, J., et al. (1997), An assessment of ozone photochemistry in the extratropical western North Pacific: Impact of continental outflow during the late winter/early spring, *J. Geophys. Res.*, *102*(D23), 28,469–28,488.

Davis, D. D., et al. (1996), Assessment of ozone photochemistry in the western North Pacific as inferred from PEM-West A observations during the fall 1991, *J. Geophys. Res.*, *101*(D1), 2111–2134.

Davis, D. D., et al. (2003), An assessment of western North Pacific ozone photochemistry based on springtime observations from NASA's PEM-West B (1994) and TRACE-P (2001) field studies, *J. Geophys. Res.*, *108*(D21), 8829, doi:10.1029/2002JD003232.

DeMore, W. B., S. P. Sander, C. J. Howard, A. R. Ravishankara, D. M. Golden, C. E. Kolb, R. F. Hampson, M. J. Kurylo, and M. J. Molina (1997), Chemical kinetics and photochemical data for use in stratospheric modelling: Evaluation number 12, *JPL Publ.*, *97-4*, pp. 14–143, NASA Jet Propul. Lab., Pasadena, Calif.

Dentener, F., D. Stevenson, J. Cofala, R. Mechler, M. Amann, P. Bergamaschi, F. Raes, and R. Derwent (2005), The impact of air pollutant and methane emission controls on tropospheric ozone and radiative forcing: CTM calculations for the period 1990–2030, *Atmos. Chem. Phys.*, *5*, 1731–1755.

Derwent, R. G., P. G. Simmonds, S. Seuring, and C. Dimmer (1998), Observation and interpretation of the seasonal cycles in the surface concentrations of ozone and carbon monoxide at Mace Head, Ireland from 1990 to 1994, *J. Atmos. Chem.*, *32*, 145–157.

DiNunno, B., D. Davis, G. Chen, J. Crawford, J. Olson, and S. Liu (2003), An assessment of ozone photochemistry in the central/eastern North Pacific as determined from multiyear airborne field studies, *J. Geophys. Res.*, *108*(D2), 8237, doi:10.1029/2001JD001468.

Duncan, B. N., R. V. Martin, A. C. Staudt, R. Yevich, and J. A. Logan (2003), Interannual and seasonal variability of biomass burning emissions constrained by satellite observations, *J. Geophys. Res.*, *108*(D2), 4100, doi:10.1029/2002JD002378.

Dunlea, E. J., and A. R. Ravishankara (2004), Measurements of the rate coefficient for the reaction of O (^{1}D) with H_2O and re-evaluation of the atmospheric OH production rate, *Phys. Chem. Chem. Phys.*, *6*, 3333–3340.

Fehsenfeld, F. C., P. Daum, W. R. Leaitch, M. Trainer, D. D. Parrish, and G. Hübler (1996), Transport and processing of O_3 and O_3 precursors over the North Atlantic: An overview of the 1993 North Atlantic Regional Experiment (NARE) summer intensive, *J. Geophys. Res.*, *101*, 28,877–28,892.

Fiore, A. M., D. J. Jacob, I. Bey, R. M. Yantosca, B. D. Field, A. C. Fusco, and J. G. Wilkinson (2002), Background ozone over the United States in summer: Origin, trend, and contribution to pollution episodes, *J. Geophys. Res.*, *107*(D15), 4275, doi:10.1029/2001JD000982.

Folkins, I., R. Chatfield, D. Baumgardner, and M. Proffitt (1997), Biomass burning and deep convection in southeastern Asia: Results from ASHOE/MAESA, *J. Geophys. Res.*, *102*, 13,291–13,300.

Gerbig, C., S. Schmitgen, D. Kley, A. Volz-Thomas, K. Dewey, and D. Haaks (1999), An improved fast-response vacuum-UV resonance fluorescence CO instrument, *J. Geophys. Res.*, *104*(D1), 1699–1704.

Grewe, V., D. Brunner, M. Dameris, J. L. Grenfell, R. Hein, D. Shindell, and J. Staehelin (2001), Origin and variability of upper tropospheric nitrogen oxides and ozone at northern mid-latitudes, *Atmos. Environ.*, *35*, 3421–3433.

Guerova, G., I. Bey, J.-L. Attié, R. V. Martin, J. Cui, and M. Sprenger (2006), Impact of transatlantic transport episodes on summertime ozone in Europe, *Atmos. Chem. Phys.*, *6*, 2057–2072.

Hannan, J. R., H. E. Fuelberg, J. H. Crawford, G. W. Sachse, and D. R. Blake (2003), Role of wave cyclones in transporting boundary layer air to the free troposphere during the spring 2001 NASA/TRACE-P experiment, *J. Geophys. Res.*, *108*(D20), 8785, doi:10.1029/2002JD003105.

Heald, C. L., et al. (2003), Asian outflow and trans-Pacific transport of carbon monoxide and ozone pollution: An integrated satellite, aircraft, and model perspective, *J. Geophys. Res.*, *108*(D24), 4804, doi:10.1029/2003JD003507.

Heald, C. L., D. J. Jacob, D. B. A. Jones, P. I. Palmer, J. A. Logan, D. G. Streets, G. W. Sachse, J. C. Gille, R. N. Hoffman, and T. Nehrkorn (2004), Comparative inverse analysis of satellite (MOPITT) and aircraft (TRACE-P) observations to estimate Asian sources of carbon monoxide, *J. Geophys. Res.*, *109*, D23306, doi:10.1029/2004JD005185.

Honrath, R. E., R. C. Owen, M. Val Martin, J. S. Reid, K. Lapina, P. Fialho, M. P. Dziobak, J. Kleissl, and D. L. Westphal (2004), Regional and hemispheric impacts of anthropogenic and biomass burning emissions on summertime CO and O_3 in the North Atlantic lower free troposphere, *J. Geophys. Res.*, *109*, D24310, doi:10.1029/2004JD005147.

Horowitz, L. W., J. Liang, G. M. Gardner, and D. J. Jacob (1998), Export of reactive nitrogen from North America during summertime: Sensitivity to hydrocarbon chemistry, *J. Geophys. Res.*, *103*, 13,451–13,476.

Horowitz, L. W., et al. (2003), A global simulation of tropospheric ozone and related tracers: Description and evaluation of MOZART, version 2, *J. Geophys. Res.*, *108*(D24), 4784, doi:10.1029/2002JD002853.

Hudman, R. C., et al. (2004), Ozone production in transpacific Asian pollution plumes and implications for ozone air quality in California, *J. Geophys. Res.*, *109*, D23S10, doi:10.1029/2004JD004974.

Huntrieser, H., et al. (2005), Intercontinental air pollution transport from North America to Europe: Experimental evidence from airborne measurements and surface observations, *J. Geophys. Res.*, *110*, D01305, doi:10.1029/2004JD005045.

Jacob, D. J. (2000), Heterogeneous chemistry and tropospheric ozone, *Atmos. Environ.*, *34*, 2131–2159.

Jacob, D. J., et al. (1996), Origin of ozone and NO_x in the tropical troposphere: a photochemical analysis of aircraft observations over the South Atlantic Basin, *J. Geophys. Res.*, *101*, 24,235–24,350.

Jacob, D. J., J. H. Crawford, M. M. Kleb, V. S. Connors, R. J. Bendura, J. L. Raper, G. W. Sachse, J. C. Gille, L. Emmons, and C. L. Heald (2003), Transport and Chemical Evolution over the Pacific (TRACE-P) aircraft mission: Design, execution, and first results, *J. Geophys. Res.*, *108*(D20), 9000, doi:10.1029/2002JD003276.

Jaeglé, L., D. J. Jacob, W. H. Brune, D. Tan, I. Faloona, A. J. Weinheimer, B. A. Ridley, T. L. Campos, and G. W. Sachse (1998), Sources of HO_x and production of ozone in the upper troposphere over the United States, *Geophys. Res. Lett.*, *25*, 1705–1708.

Jaffe, D., et al. (1999), Transport of Asian air pollution to North America, *Geophys. Res. Lett.*, *26*, 711–714.

Jaffe, D., I. McKendry, T. Anderson, and H. Price (2003), Six new episodes of trans-Pacific transport of air pollutants, *Atmos. Environ.*, *37*, 391–404.

Kondo, Y., et al. (2004), Impacts of biomass burning in Southeast Asia on ozone and reactive nitrogen over the western Pacific in spring, *J. Geophys. Res.*, *109*, D15S12, doi:10.1029/2003JD004203.

Li, Q. B., et al. (2002a), Transatlantic transport of pollution and its effects on surface ozone in Europe and North America, *J. Geophys. Res.*, *107*(D13), 4166, doi:10.1029/2001JD001422.

Li, Q. B., D. J. Jacob, T. D. Fairlie, H. Y. Liu, R. M. Yantosca, and R. V. Martin (2002b), Stratospheric versus pollution influences on ozone at Bermuda: Reconciling past analyses, *J. Geophys. Res.*, *107*(D22), 4611, doi:10.1029/2002JD002138.

Li, Q. B., D. J. Jacob, R. Park, Y. Wang, C. L. Heald, R. Hudman, R. M. Yantosca, R. V. Martin, and M. Evans (2005), North American pollution outflow and the trapping of convectively lifted pollution by upper-level anticyclone, *J. Geophys. Res.*, *110*, D10301, doi:10.1029/2004JD005039.

Liang, Q., L. Jaeglé, D. A. Jaffe, P. Weiss, A. Heckman, and J. Snow (2004), Long-range Transport to the Northeast Pacific: Seasonal variations and transport pathways, *J. Geophys. Res.*, *109*, D23S07, doi:10.1029/2003JD004402.

Lin, S.-J., and R. B. Rood (1996), Multidimensional flux form semi Lagrangian transport schemes, *Mon. Weather Rev.*, *124*, 2046–2070.

Liu, H., D. J. Jacob, L. Y. Chan, S. J. Oltmans, I. Bey, R. M. Yantosca, J. M. Harris, B. N. Duncan, and R. V. Martin (2002), Sources of tropospheric ozone along the Asian Pacific Rim: An analysis of ozonesonde observations, *J. Geophys. Res.*, *107*(D21), 4573, doi:10.1029/2001JD002005.

Liu, H., D. J. Jacob, I. Bey, R. M. Yantosca, B. N. Duncan, and G. W. Sachse (2003), Transport pathways for Asian pollution outflow over the Pacific: Interannual and seasonal variations, *J. Geophys. Res.*, *108*(D20), 8786, doi:10.1029/2002JD003102.

Logan, J. A. (1999), An analysis of ozonesonde data for the troposphere: Recommendations for testing 3-D models and development of a gridded climatology for tropospheric ozone, *J. Geophys. Res.*, *104*(D13), 16,115–16,150.

Lövblad, G., L. Tarrasón, K. Tørseth, and S. Dutchak (Eds.) (2004), EMEP Assessment, part 1: European perspective, Norw. Meteorol. Inst., Oslo.

Martin, R. V., D. J. Jacob, R. M. Yantosca, M. Chin, and P. Ginoux (2003), Global and regional decreases in tropospheric oxidants from photochemical effects of aerosols, *J. Geophys. Res.*, *108*(D3), 4097, doi:10.1029/2002JD002622.

McLinden, C. A., S. C. Olsen, B. Hannegan, O. Wild, M. J. Prather, and J. Sundet (2000), Stratospheric ozone in 3-D models: A simple chemistry and the cross-tropopause flux, *J. Geophys. Res.*, *105*, 14,653–14,665.

Naja, M., H. Akimoto, and J. Staehelin (2003), Ozone in background and photochemically aged air over central Europe: Analysis of long-term ozonesonde data from Hohenpeissenberg and Payerne, *J. Geophys. Res.*, *108*(D2), 4063, doi:10.1029/2002JD002477.

Newell, R. E., E. V. Browell, D. D. Davis, and S. C. Liu (1997), Western Pacific tropospheric ozone and potential vorticity: Implications for Asian pollution, *Geophys. Res. Lett.*, *24*, 2733–2736.

Nordeng, T. E. (1994), Extended versions of the convective parameterization scheme at ECMWF and their impact on the mean and transient activity of the model in the tropics, *Tech. Memo. 206*, Eur. Cent. for Med.-Range Weather Forecasts, Reading, U. K.

Olson, J. R., et al. (2001), Seasonal differences in the photochemistry of the South Pacific: A comparison of observations and model results from PEM-Tropics A and B, *J. Geophys. Res.*, *106*(D23), 32,749–32,766.

Ordóñez, C., H. Mathis, M. Furger, S. Henne, C. Hüglin, J. Staehelin, and A. S. H. Prévôt (2005), Changes of daily surface ozone maxima in Switzerland in all seasons from 1992 to 2002 and discussion of summer 2003, *Atmos. Chem. Phys.*, *5*, 1187–1203.

Parrish, D. D., J. S. Holloway, M. Trainer, P. C. Murphy, G. L. Forbes, and F. C. Fehenseld (1993), Export of North American ozone pollution to the North Atlantic Ocean, *Science*, *259*, 1436–1439.

Parrish, D. D., M. Trainer, J. S. Holloway, J. E. Yee, M. S. Warshawsky, F. C. Fehsenfeld, G. L. Forbes, and J. L. Moody (1998), Relationships between ozone and carbon monoxide at surface sites in the North Atlantic region, *J. Geophys. Res.*, *103*(D11), 13,357–13,376.

Parrish, D. D., et al. (2004), Changes in the photochemical environment of the temperate North Pacific troposphere in response to increased Asian emissions, *J. Geophys. Res.*, *109*, D23S18, doi:10.1029/2004JD004978.

Penkett, S., et al. (2004), Long-range transport of ozone and related pollutants over the North Atlantic in spring and summer, *Atmos. Chem. Phys. Disc.*, *4*, 4407–4454.

Pickering, K. E., Y. S. Wang, W. K. Tao, C. Price, and J. F. Muller (1998), Vertical distributions of lightning NO_x for use in regional and global chemical transport models, *J. Geophys. Res.*, *103*, 31,203–31,216.

Price, C., and D. Rind (1992), A simple lightning parameterization for calculating global lightning distributions, *J. Geophys. Res.*, *97*, 9919–9933.

Price, H. U., D. A. Jaffe, O. R. Cooper, and P. V. Doskey (2004), Photochemistry, ozone production, and dilution during long-range transport episodes from Eurasia to the northwest United States, *J. Geophys. Res.*, *109*, D23S13, doi:10.1029/2003JD004400.

Purvis, R. M., et al. (2003), Rapid uplift of nonmethane hydrocarbons in a cold front over central Europe, *J. Geophys. Res.*, *108*(D7), 4224, doi:10.1029/2002JD002521.

Randel, W. J., F. Wu, J. M. Russell, A. Roche, and J. W. Waters (1998), Seasonal cycles and QBO variations in stratospheric CH_4 and H_2O observed in UARS HALOE data, *J. Atmos. Sci.*, *55*, 163–185.

Ravishankara, A. R., E. J. Dunlea, M. A. Blitz, T. J. Dillon, D. E. Heard, M. J. Pilling, R. S. Strekowski, J. M. Nicovich, and P. H. Wine (2002), Redetermination of the rate coefficient for the reaction of O (^{1}D) with N_2, *Geophys. Res. Lett.*, *29*(15), 1745, doi:10.1029/2002GL014850.

Reeves, C. E. and the EXPORT Team, (2003) Results from EXPORT (European EXport of Precursors and Ozone by Long-Range Transport) and lessons learned, in *European Export of Particulates and Ozone by Long-Range Transport (EXPORT-E2—Final Report)*, edited by S. A. Penkett et al., pp. 147–150, Int. Sci. Secr., Munich, Germany.

Reeves, C. E., et al. (2002), Potential for photochemical ozone formation in the troposphere over the North Atlantic as derived from aircraft observations during ACSOE, *J. Geophys. Res.*, *107*(D23), 4707, doi:10.1029/2002JD002415.

Roeckner, E. et al. (2003), The atmospheric general circulation model ECHAM 5. Part I: Model description, *MPI Rep. 349*, Max Planck Inst. for Meteorol., Hamburg, Germany. (Available at http://www.mpimet.mpg.de/fileadmin/publikationen/Reports/max_scirep_349.pdf)

Sander, S. P. et al. (2000), Chemical kinetics and photochemical data for use in stratospheric modelling: Supplement to evaluation number 12: Evaluation number 13, *JPL Publ.*, *00–3*, pp. 10–28, NASA Jet Propul. Lab., Pasadena, Calif.

Schneider, H. R., D. B. A. Jones, M. B. McElroy, and G.-Y. Shi (2000), Analysis of residual mean transport in the stratosphere 1. Model description and comparison with satellite data, *J. Geophys. Res.*, *105*(D15), 19,991–20,012.

Schultz, M., R. Schmitt, K. Thomas, and A. Volz-Thomas (1998), Photochemical box modeling of long-range transport from North America to Tenerife during the North Atlantic Regional Experiment (NARE) 1993, *J. Geophys. Res.*, *103*(D11), 13,477–13,488.

Schultz, M., et al. (1999), On the origin of tropospheric ozone and NO_x over the tropical Pacific, *J. Geophys. Res*, *104*, 5829–5844.

Simmonds, P. G., R. G. Derwent, A. L. Manning, and G. Spain (2004), Significant growth in surface ozone at Mace Head, Ireland, 1987–2003, *Atmos. Environ.*, *38*, 4769–4778.

Stevenson, D. S., et al. (2006), Multimodel ensemble simulations of present-day and near-future tropospheric ozone, *J. Geophys. Res.*, *111*, D08301, doi:10.1029/2005JD006338.

Stohl, A. (2001), A 1-year Lagrangian climatology of airstreams in the Northern Hemisphere troposphere and lowermost stratosphere, *J. Geophys. Res.*, *106*, 7263–7280.

Stohl, A., and T. Trickl (1999), A textbook example of long-range transport: Simultaneous observation of ozone maxima of stratospheric and North American origin in the free troposphere over Europe, *J. Geophys. Res.*, *104*, 30,445–30,462.

Thompson, A. M., K. E. Pickering, R. R. Dickerson, W. G. Ellis, D. J. Jacob, J. R. Scala, W.-K. Tao, D. P. McNamara, and J. Simpson (1994), Convective transport over the central United States and its role in regional CO and ozone budgets, *J. Geophys. Res.*, *99*, 18,703–18,712.

Tie, X., S. Madronich, S. Walters, D. P. Edwards, P. Ginoux, N. Mahowald, R. Zhang, C. Lou, and G. Brasseur (2005), Assessment of the global impact of aerosols on tropospheric oxidants, *J. Geophys. Res.*, *110*, D03204, doi:10.1029/2004JD005359.

Tiedtke, M. (1989), A comprehensive mass flux scheme for cumulus parameterization in large-scale models, *Mon. Weather Rev.*, *117*, 1779–1800.

Trickl, T., O. R. Cooper, H. Eisele, P. James, R. Mücke, and A. Stohl (2003), Intercontinental transport and its influence on the ozone concentrations over central Europe: Three case studies, *J. Geophys. Res.*, *108*(D12), 8530, doi:10.1029/2002JD002735.

van der Werf, G. R., J. T. Randerson, G. J. Collatz, and L. Giglio (2003), Carbon emissions from fires in tropical and subtropical ecosystems, *Global Change Biol.*, *9*, 547–562.

Wang, Y., D. J. Jacob, and J. A. Logan (1998), Global simulation of tropospheric O_3-NO_x-hydrocarbon chemistry: 1, Model formulation, *J. Geophys. Res.*, *103*, 10,713–10,726.

Wild, O., and H. Akimoto (2001), Intercontinental transport of ozone and its precursors in a three-dimensional global CTM, *J. Geophys. Res.*, *106*, 27,729–27,744.

Wild, O., K. S. Law, D. S. McKenna, B. J. Bandy, S. A. Penkett, and J. A. Pyle (1996), Photochemical trajectory modeling studies of the North Atlantic region during August 1993, *J. Geophys. Res.*, *101*(D22), 29,269–29,288.

Wild, O., X. Zhu, and M. J. Prather (2000), Fast-J: Accurate simulation of in- and below-cloud photolysis in tropospheric chemistry models, *J. Atmos. Chem.*, *37*, 245–282.

Wild, O., et al. (2004), Chemical transport model ozone simulations for spring 2001 over the western Pacific: Regional ozone production and its global impacts, *J. Geophys. Res.*, *109*, D15S02, doi:10.1029/2003JD004041.

Yienger, J., M. Galanter, T. A. Holloway, M. J. Phadnis, S. K. Guttikunda, G. R. Carmichael, W. J. Moxim, and H. Levy II (2000), The episodic nature of air pollution transport from Asia to North America, *J. Geophys. Res.*, *105*, 26,931–26,946.

M. Auvray and I. Bey, Laboratoire de Modélisation de la Chimie Atmosphérique, Ecole Polytechnique Fédérale de Lausanne, Station 2, CH-1015 Lausanne, Switzerland. (marion.auvray@epfl.ch; isabelle.bey@epfl.ch)

E. Llull, Department of Geosciences, University of Fribourg, Ch. Du Musée 4, CH-1700 Fribourg, Switzerland. (eric.llull@unifr.ch)

S. Rast and M. G. Schultz, Max Planck Institute for Meteorology, Bundesstr. 53, D-20146 Hamburg, Germany. (rast@dkrz.de; martin.schultz@dkrz.de)